

FoxN3 knock-down alters spatio-temporal expression patterns of genes involved in cranial cartilage and muscle development in the African clawed-frog *Xenopus laevis*

JENNIFER SCHMIDT^{1,*}, MAXIMILIAN SCHUFF², BENJAMIN NAUMANN¹ & LENNART OLSSON^{1,*}

¹ Institut für Zoologie und Evolutionsforschung, Friedrich-Schiller-Universität, Erbertstraße 1, 07743 Jena, Germany; jenniferschmidt2012@hotmail.com, lennart.olsson@uni-jena.de — ² IVF Zentren Prof. Zech – Bregenz GmbH, Römerstraße 2/4, 6900 Bregenz, Austria — * Corresponding authors

Submitted May 19, 2020.

Accepted August 12, 2020.

Published online at www.senckenberg.de/vertebrate-zoology on September 9, 2020.

Published in print Q3/2020.

Editor in charge: Ingmar Werneburg

Abstract

What is the gene regulatory network underlying the morphogenesis of the vertebrate head skeleton? A good candidate to approach this question is the *FoxN3* gene. Morpholino-mediated FoxN3 knock-down leads to a delay in cranial cartilage and muscle formation, to reduced size and to malformations of both cartilages and muscles in *Xenopus laevis*. Additionally, muscle fiber development and joint formation are incomplete. We used qRT-PCR and whole-mount *in situ* hybridization to analyse potential target genes of *FoxN3*. The spatio-temporal expressions of different cartilage, muscle, and joint markers as well as cell adhesion molecules are changed following *FoxN3* knock-down. Expression of *N-CAM* and *N-Cad* is decreased throughout development and expression of genes important for cartilage formation (*Sox9*, *Col2a1*, *Runx2*) is delayed. Joint markers (*Gdf5/6*) and genes (*Dlx5/6*) important for regional specification are also down-regulated and *bagpipe* genes show decreased expression at consecutive stages. Expression levels of key myogenic genes (*Myf5*, *MyoD*, *MHC*) are at 30–40% of control expression. These results indicate that *FoxN3* occupies a key position in the gene regulatory network maintaining normal development of cranial cartilages and muscles as well as jaw joint formation.

Key words

Chondrogenesis, forkhead transcription factor, HDAC, myogenesis, neural crest.

Introduction

What are the genes and genetic interactions controlling the exact positioning and morphogenesis of the vertebrate head skeleton and its associated musculature? The key to approach this question and to elucidate the evolutionary origin of the vertebrate head in general is an embryonic cell population called cranial neural crest cells (cNCCs) (HALL, 2009). Since GANS & NORTHCUTT'S (1983) "New Head hypothesis" the development and migration of the cNCCs has gained much attention. Vertebrate cNCCs contribute to cranial cartilages and bones (HALL, 2009) and to the connective tissue of jaw and branchial muscles (LE LIÈVRE & LE DOUARIN, 1975; NODEN, 1983; COULY

et al., 1992; LE DOUARIN *et al.*, 1993; OLSSON *et al.*, 2001; ERICSSON *et al.*, 2004). Although the delamination and migration of cNCCs has been well characterized, the complex gene regulatory network orchestrating cartilage and muscle differentiation and morphogenesis is still insufficiently understood.

Cartilage development is a multi-step process that starts with epithelial-mesenchymal interactions followed by condensation, proliferation and differentiation (reviewed in HALL, 2005). Epithelial-mesenchymal interactions are important for the localization of embryonic skeletal elements, maintenance of skeletal progenitor cells,

the initiation of mesenchymal condensation and the onset of differentiation. Subsequent steps in chondrogenesis may either be delayed or not initiated if condensations fail to attain a critical size, resulting in severe skeletal malformations (HALL & MIYAKE, 1992). The aggregation of mesenchymal cells into precartilaginous tissue depends upon signals initiated by cell-cell and cell-matrix interactions (HALL, 2005). This process is associated with increasing cell adhesion, establishment of boundaries, formation of gap junctions and changes in cytoskeletal architecture, proliferation and three-dimensional growth (HALL & MIYAKE, 1995).

The onset of condensation is marked by cell adhesion molecules, such as the *neural cell adhesion molecule (N-CAM)* and *neural cadherin (N-Cad)* (HALL, 2005). After condensations are established, the *bone morphogenetic protein2, 4 and 7 (BMP2, 4 and 7)* orchestrate the generation of cartilage boundaries and thereby determine condensation size (HALL, 2009). Transcription factors such as *runt-related transcription factor 2 (Runx2)* and *sex determining region Y-box 9 (Sox9)* modulate cell proliferation within these condensations (GOLDRING *et al.*, 2006). Differentiation is initiated by a down-regulation of cell adhesion molecules through BMPs, the activation of homeobox genes [e.g., *Msh homeobox 1 and 2 (Msx1 and Msx2)*] and increased synthesis of extracellular matrix proteins, mainly collagen II and IX (HALL & MIYAKE, 1992, 1995) from genes like *Collagen 2 alpha 1 (Col2a1)*. The process of joint formation is tightly connected to cartilage formation. With the formation of cartilage condensations an intermediate domain is maintained that later develops to the joint capsule. In the intermediate domain several genes are expressed, such as *BMP4*, *growth differentiation factor 5 (Gdf5)* and *Xenopus bagpipe (Xbp)*, while *Sox9* expression is decreased (SATO *et al.*, 2005; LUKAS & OLSSON, 2018b).

Additionally, the development of NC (neural crest)-derived structures in the head, including connective tissues and cartilages, are important for correct muscle development. Several studies have shown that migration, patterning and differentiation of muscle precursors are regulated by cNCCs (NODEN, 1983; LE DOUARIN *et al.*, 1993; OLSSON *et al.*, 2001; GRENIER *et al.*, 2009). cNCCs provide the scaffold for proper extension of the cranial muscles and subsequent attachment to the correct cartilages (ERICSSON *et al.*, 2004). The absence of cNCCs results in myoblasts failing to undergo terminal differentiation (RINON *et al.*, 2007). Genes like *myoblast determination protein (MyoD)*, *myogenic factor 5 (Myf5)*, *myogenin*, *myogenic regulatory factor 4 (MRF4)*, *musculin (MyoR)* and *Capsulin* exert diverse roles during muscle development and make up the myogenic core program. *MRF4*, *MyoR* and *Capsulin* specifically influence the rate of cell proliferation and differentiation within this myogenic core program (HOPWOOD *et al.*, 1991, 1992; LU *et al.*, 2002; CHANOINE & HARDY, 2003; ERICSSON *et al.*, 2009).

FoxN3, a member of the *forkhead/winged helix* gene family of transcription factors, is important for normal

development of NC-derived cartilages and proper cranial muscle patterning in *Xenopus laevis* DAUDIN, 1802 (SCHUFF *et al.*, 2007; SCHMIDT *et al.*, 2011, 2013). Morpholino-mediated knock-down of *FoxN3* results in abnormal formation of the jaw cartilages and jaw joints, and in loss or shortening of skeletal processes (Figure 1; for details see SCHUFF *et al.*, 2007 and SCHMIDT *et al.*, 2011, 2013). Both cartilage and muscle development is delayed, progenitor condensations are smaller, muscles fuse and appear to have shortened and frayed ends (SCHMIDT *et al.*, 2011, 2013). Due to these large-scale effects *FoxN3* seems to be a promising candidate to detangle the gene regulatory network underlying the “normal” development of the vertebrate head.

In this study, we investigate the spatio-temporal expression patterns of genes involved in chondrogenesis and myogenesis in “normal” (control) and *FoxN3* depleted *X. laevis* embryos. We show that Morpholino-mediated knock-down of *FoxN3* causes delayed and spatially decreased expression levels of key cartilage and muscle markers. These changes at the molecular level can explain the phenotypic effects documented in our previous studies (SCHUFF *et al.*, 2007; SCHMIDT *et al.*, 2011, 2013).

Materials and methods

Database analyses and alignments

The following programs were used for Expressed Sequence Tags and comparative genomic analyses of gene homologues and primer pairs: NCBI <http://www.ncbi.nlm.nih.gov/blast>, <http://www.ensembl.org/index.html>, and <http://www.ebi.ac.uk/Tools/clustalw>.

Specimens

Xenopus laevis eggs were obtained from breeding colonies of the universities in Ulm and Jena between 2012 and 2014. Spawning was induced by injecting 600 units of human chorionic gonadotropin in the dorsal lymph sac of female and 200 units in the dorsal lymph sac of male frogs. Fertilized eggs were collected and cultured in 0.1 × MBSH (1 × MBSH; 88 mM NaCl, 2.4 mM NaHCO₃, 0.82 mM MgSO₄, 0.41 mM CaCl₂, 0.33 mM Ca(NO₃)₂, 10 mM HEPES, pH 7.4) until the stage of interest. Staging was according to the normal table of (NIEUWKOOP & FABER, 1994). All experiments were carried out according to the animal welfare protocols at Friedrich Schiller University Jena.

Morpholino injections

A *FoxN3* Morpholino antisense oligonucleotide (*FoxN3-Mo*) was derived from the first 25 nucleotides of

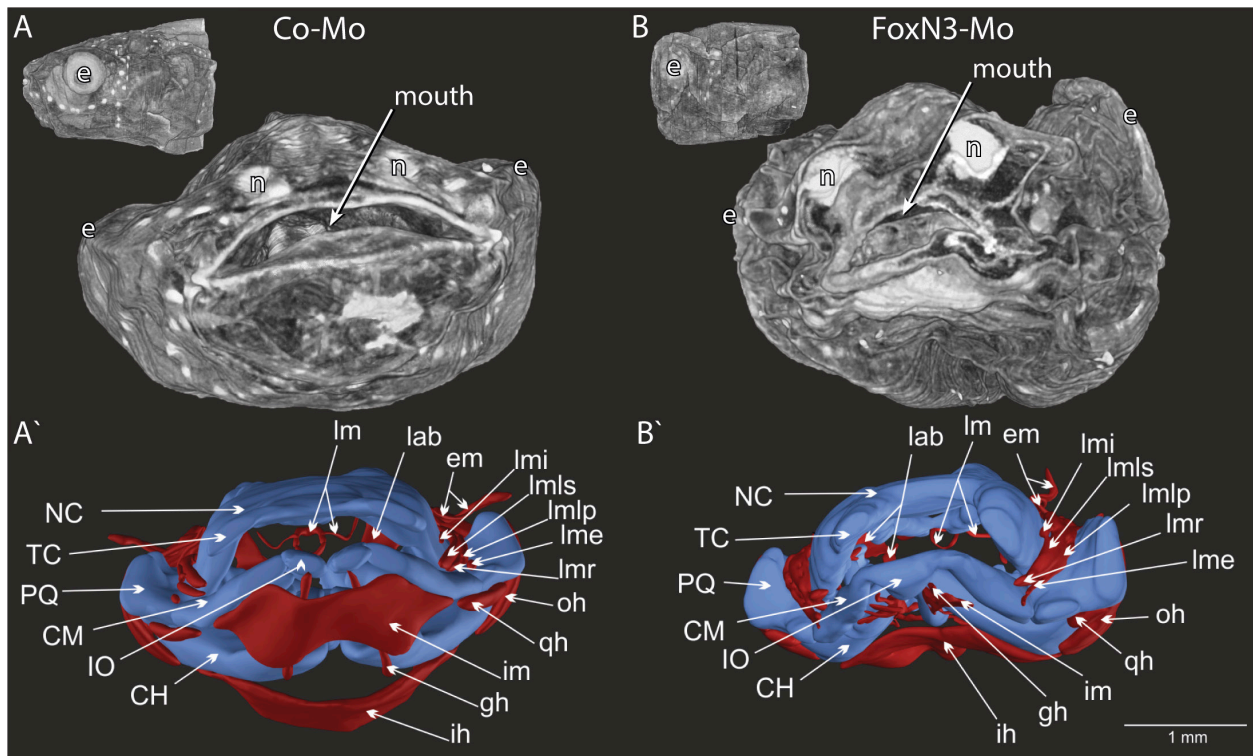


Fig. 1. Craniofacial malformations after FoxN3 knock-down in *Xenopus laevis* larvae at stage 46. A, A', Co-Mo bilaterally injected. A, volume rendering. The lateral view is shown in the top right corner, the frontal view in the middle. A', Three-dimensional reconstructions of the cranial skeleton (blue) and muscles (dark red). B, B', FoxN3-Mo bilaterally injected. B, volume rendering. The lateral view is shown in the top right corner, the frontal view in the middle. B', Three-dimensional reconstructions of the cranial skeleton (blue) and muscles (dark red). Cartilages: CH, ceratohyal; CM, Meckel's cartilage; e, eye; em, eye muscles; gh, m. geniohyoideus; ih, m. interhyoideus; im, m. intermandibularis; IR, infrastrahl; lab, mm. levator arcuum branchialium I-IV; lm, laryngeal muscles; lme, m. levator mandibulae externus; lmi, m. levator mandibulae internus; lmlp, m. levator mandibulae longus profundus; lmls, m. levator mandibulae longus superior; lmr, m. levator mandibulae anterior; n, nostril; NC, Neurocranium; oh, m. orbitohyoideus; PQ, palatoquadrate; qh, m. quadrato-hyoangularis; TC, trabeculae cranii.

the translation start of the *FoxN3* gene (5'-ACTAG-GAGGGCATGACTGGACCCAT-3'; Gene Tools, USA) as previously described (SCHUFF *et al.*, 2007). Specificity of the used Morpholino was previously verified (SCHUFF *et al.*, 2006). Morpholino injections were performed in 4% Ficoll / 0.5 × MBSH. FoxN3-Mo was injected in doses of 15–17 ng into one or two blastomeres of two cell stage embryos. For control a Morpholino oligonucleotide (Co-Mo) against the sequence of the human β -globin gene (5'-CCTCTTACCTCAGTTACAATTATA-3'; Gene Tools, USA) was injected under identical conditions. Non-injected controls were used to screen the eggs for normal development.

Quantitative real time-PCR (qRT-PCR)

QiaZol (Qiagen) was used to extract total RNA from collected *FoxN3* depleted as well as control tadpoles of different developmental stages. RNA was subjected to DNase I treatment and purified by using the RNeasy kit (Qiagen). First strand cDNA was synthesized from 2 g of total RNA with RevertAid™ First Strand cDNA Synthesis kit (Fermentas). The fluorescence-based quantitative

real-time PCR (qRT-PCR) reactions were done according to the QuantiTect™ SYBR Green PCR handbook (Qiagen) in a total volume of 20 μ l, containing 10 μ l of the QuantiTect™ SYBR Green PCR Master Mix (Qiagen), 0.5 μ l of each primer (10 pmol/ μ l) and 2 μ l of 1:10 diluted template cDNA. The qPCR reactions for the genes *N-CAM*, *N-Cad*, *Dlx5*, *Dlx6*, *Gdf5*, *Gdf6* and *XMyf5* were done according to the KAPA™SYBR®FAST handbook (peqlab) in a total volume of 20 μ l, containing 2.5 μ l of the KAPA™SYBR®FAST qPCR MasterMix (2×) Universal (peqlab), 0.25 μ l of the ROX Reference Dye Low (50x) (peqlab), 0.5 μ l of each primer (10 pmol/ μ l) and 1 μ l of 1:10 diluted template cDNA. The gene-specific primers used and the cycling conditions are listed in Supplementary material 1. For negative control, a no template (water) control and RT- probe (without RNA template) were used. The quantification cycle (C_q) in log-linear phase of amplification and the PCR efficiency was quantified by using LightCycler™ software version 1.0 (Roche) for the first genes mentioned. For the second group the MxPro software version Mx3005P v4.01 Build 369, Schema 80 (Stratagen) was used. Values were normalized to the expression level of the reference gene *H4* (*histone4*). This was done in each run for each sample in-

cluding RT- and water using $\Delta\Delta Ct$ -method. The H4 variation was minimized by including it in each run and each sample and the variation over the three replicates was in average 0.045. Each run was further controlled by analysis of the dsDNA melting curve at the end of each PCR as well as a control of the resulting amplicates via gel electrophoresis. The expression of each gene in whole body and only the head region was calculated relative to Co-Mo (Control-Morpholino) injected larvae, in which gene expression was considered as basal level. Co-Mo injected specimens were used for analyses to account the injection at itself as manipulation and to be aware of artefacts due to injection. For biostatistical analysis a student t-test for the three independent biological replicates was used with a confidence interval of 95% and data is presented in histograms as relative units. According to the sample maximization method all three replicates of a samples of the same stage and the same gene are analysed in the same experiment to minimize run-to run variations (for details see DERVEAUX *et al.*, 2010). Experiments were repeated at least three times.

In situ-hybridization

Five to ten tadpoles per gene at the stages 31/32, 33/34, 35/36, 37/38, 39, 41 and 45 were used for whole mount *in situ* hybridization. Two to five tadpoles of selected stages and genes were used for serial sectioning for a histological analysis of the expression domains. Larvae were anesthetized with 3-aminobenzoic acid ethyl ester (MS222; Sigma, St. Louis, MO) and fixed using 4% phosphate buffered paraformaldehyde (PFA) or MEMFA (0,1 M MOPS, pH 7.4; 2mM EGTA; 1mM MgSO₄; 4% PFA). For investigation of expression levels, we used a triple independent setup. In three independent injection experiments, ten FoxN3-Mo injected tadpoles at stages 25, 30, 34, 38, 42 and 45, as well as ten control tadpoles from the same clutch, were collected, anesthetized, immediately frozen using liquid nitrogen and stored at -80°C for maximum one week. For serial sectioning, tadpoles at stage 31/32 and 33/34 were embedded in Technovit 8100 and for stages 35/36, 37/38, 39, 41 and 45 in paraffin according to (ROMEIS, 2007) and sections of 3 or 7 μm thickness were produced using a rotary microtome (HM360 Microm, Germany). Additionally, paraffin sections were used for *in situ* hybridization according to (HARLAND, 1991) with some modifications (First day: 10 min 99% Ethanol, 5 min 75% Ethanol/25% DEPC-H₂O, 5 min 50% Ethanol/50% DEPC-H₂O, 5 min 25% Ethanol/75% DEPC-H₂O, wash 3×5 min 100% PTW, 8 min 0,5 μl Proteinase K/ml 100% PTW at 37°C , 5 min 0.1 M Triethanolamin (pH7.8), 10 min 0.1 M Triethanolamin (pH7.8) + Acetic Anhydride (0.5 $\mu\text{l}/\text{ml}$), 2×5 min 100% PTW, 20 min 4% PFA, 3×5 min 100% PTW, 1 h Hyb. Buffer (1 mg/ml Chaps, $5 \times$ SSC, 50 mg/ml yeast RNA, 50 mg/ml Heparin, 5xDenhardts, 10% Tween-20, 5% 0.2 M EDTA, 50% Formamid) at 63°C , 6 h Hybridization Buffer containing 10 $\mu\text{g}/\text{ml}$ DIG labelled probe at

63°C , 10 min Hybridization Buffer, 3×5 min $2 \times$ SSC at 63°C , 3×5 min $0.2 \times$ SSC at 63°C , 2×5 min MNT, 1 h Blocking Buffer (2% Blocking Reagent (Roche), 20% lamb-Serum, 200 mM C₄H₄O₄, 300 mM NaCl, 10% Tween-20) and afterwards Blocking Buffer + 1/2000 DIG-AK over night at 4°C ; Second day: wash 4×5 min MNT, 2×10 min AP Buffer, cover slide with 10–20 μl BMP-purple until staining in the dark). For whole mount *in situ* hybridization, plasmids were linearized and transcribed with T7-, Sp6- and T3-RNA polymerase to generate antisense RNA probes using Boehringer-DIG Kit (Roche). Images of cross sections were obtained with an Axioplan microscope (Zeiss, Germany) in conjunction with a colorView12 camera (Olympus Soft Imaging System, Germany) using the program AnalySIS[®]3.2 (Olympus Soft Imaging System). Images of whole-mount stained larvae were acquired with a Stemi SV11 stereo microscope (Zeiss, Germany) with a colorViewIII camera (Olympus Soft Imaging System) and AnalySIS[®]3.2.

3D-reconstruction

The three-dimensional reconstructions were based on X-ray- μCT scans of *X. laevis* tadpoles (stage 46) injected bilaterally with 15 ng FoxN3-MO, and of Co-Mo injected controls, using the Xradia MicroXCT system at the Dept. of Theoretical Biology, University of Vienna. BITPLAN IMARIS 6.1.5 software (Bitplan AG, Switzerland) was used to create the surface structures which were further transferred to Alias[®] MAYA 7.0 software (Alias Wavefront, Canada). The single surface data were assembled and smoothed to eliminate surface artefacts, with no relevant changes in arrangement and general shape.

Results

Morpholino-mediated knock-down of FoxN3 alters spatio-temporal expression patterns of genes involved in cranial chondrogenesis

For all genes, the temporal gene expression levels in FoxN3-depleted specimens are compared to specimens injected with the Co-Mo (controls). In the following the results are presented as changes in expression: quantitative (bar charts, decrease, increase, unchanged) and qualitative (*in situ* hybridisations).

N-CAM (Figure 2A) – stage 25, slightly decreased; stage 30, significant decrease ($p=0.022$); stage 34, slightly decreased; stage 38, significant increase ($p=0.001$); stage 42, slightly decreased; stage 45, significantly decreased ($p=0.017$).

N-Cad (Figure 2A) – stage 25, slightly decreased; stage 30, unchanged; stage 34, slightly decreased; stage 38,

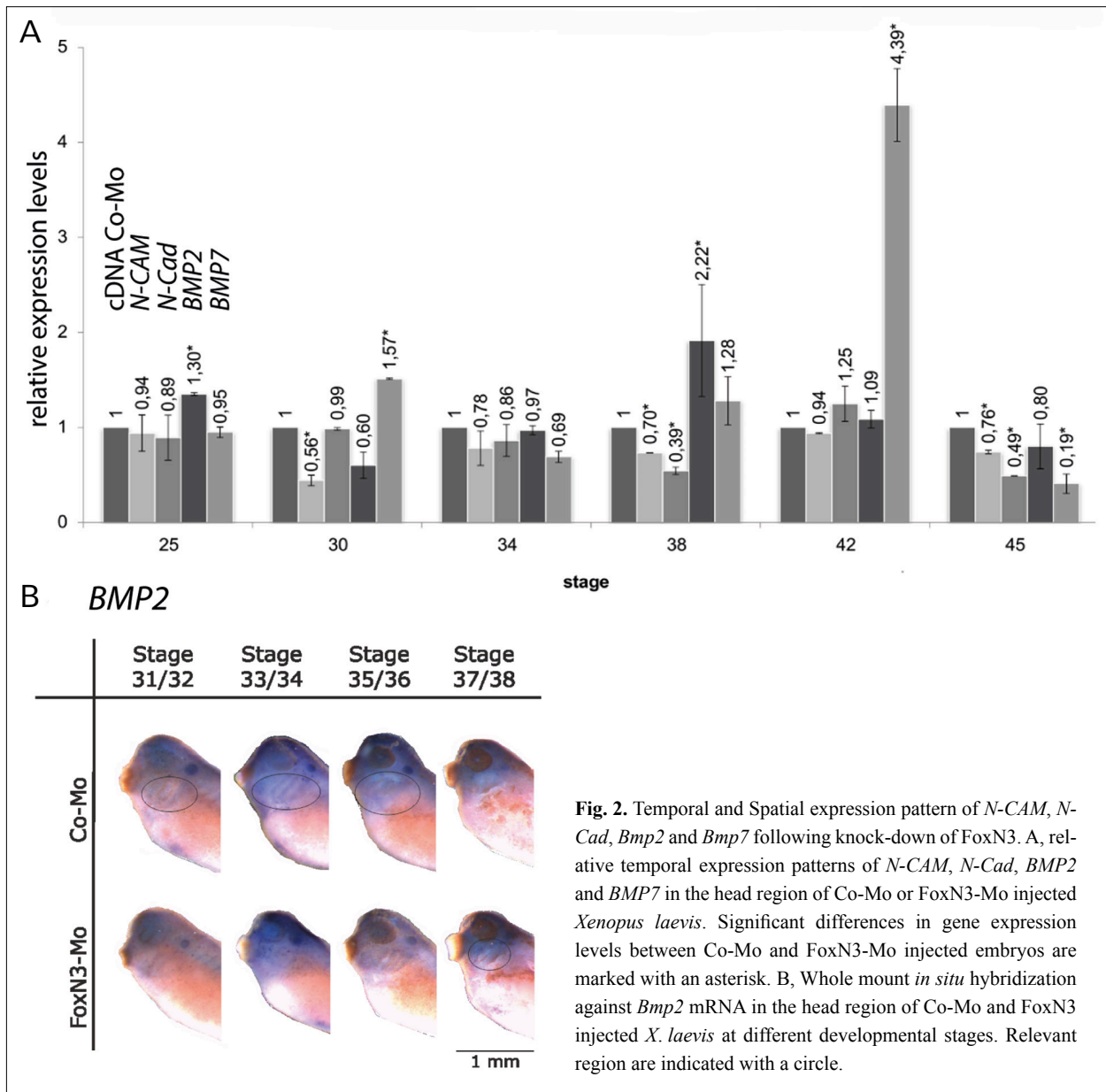


Fig. 2. Temporal and Spatial expression pattern of *N-CAM*, *N-Cad*, *Bmp2* and *Bmp7* following knock-down of FoxN3. A, relative temporal expression patterns of *N-CAM*, *N-Cad*, *BMP2* and *BMP7* in the head region of Co-Mo or FoxN3-Mo injected *Xenopus laevis*. Significant differences in gene expression levels between Co-Mo and FoxN3-Mo injected embryos are marked with an asterisk. B, Whole mount *in situ* hybridization against *Bmp2* mRNA in the head region of Co-Mo and FoxN3 injected *X. laevis* at different developmental stages. Relevant region are indicated with a circle.

significant 2.5 fold increase ($p=0,024$); stage 42, slightly increased; stage 45, significant 0.5 fold decrease.

BMP2 (Figure 2A) – stage 25, significant 1.3 fold increase ($p=0.01$); stage 30, significantly decreased ($p=0.021$); stage 34, unchanged; stage 38, significant 2.2 fold increase ($p=0.04$); stage 42, unchanged; stage 45, slightly decreased.

In situ hybridization against *BMP2* reveals a slightly condensed spatial expression in the developing facial and branchial regions of FoxN3-depleted specimens between stage 31 and 36 compared to controls (Figure 2B). At stage 37/38, staining is more intense and more condensed in FoxN3-depleted specimens (Figure 2B). This pattern matches the alterations in temporal expression levels observed in the qRT-PCR data.

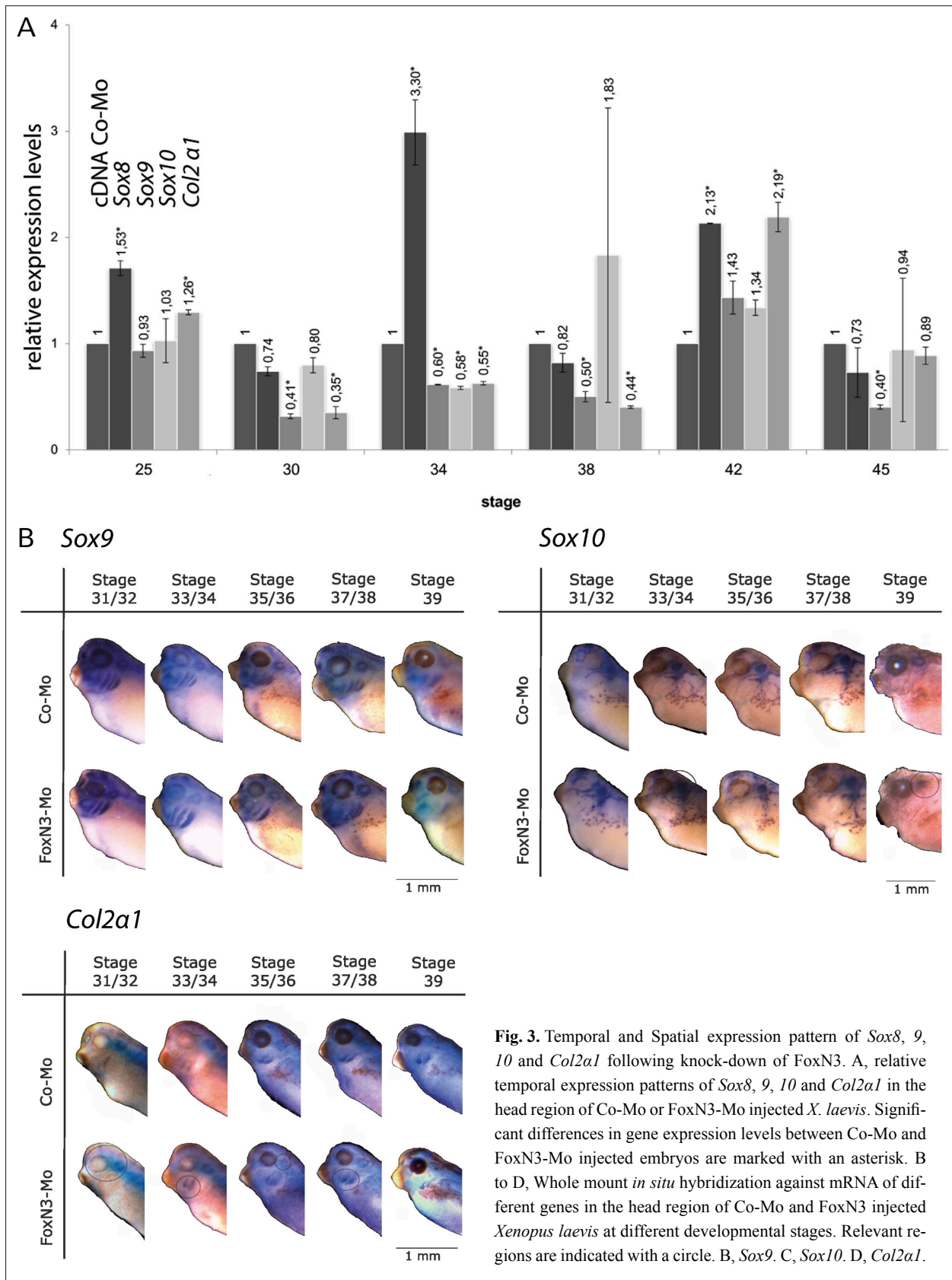
BMP7 (Figure 2A) – stage 25, unchanged; stage 30, significant increase ($p=0.017$); stage 34, slightly decreased;

stage 38, slightly increased; stage 42, significant 4.4 fold increase ($p=0.02$); stage 45, significant 0.5 fold decrease ($p=0.01$).

Sox8 (Figure 3A) – stage 25, significantly increased ($p=0.015$); stage 30, slightly decreased; stage 34, significant threefold increase ($p=0.0058$); stage 38, slightly decreased; stage 42, significant twofold increase ($p=0.001$); stage 45, slightly decreased.

Sox9 (Figure 3A) – stage 25, slightly decreased; stage 30, significantly decreased ($p=0.0024$); stage 34, significantly decreased ($p=0.0005$); stage 38, significantly decreased ($p=0.004$); stage 42, slightly increased; stage 45, significantly decreased ($p=0.0001$).

In situ hybridization against *Sox9* in different developmental stages of FoxN3-depleted specimens reveals an unchanged spatial expression pattern compared to controls. *Sox9* is expressed in the developing jaw, branchial



region, neurocranium and otic capsule (Figure 3B). The intensity of the staining varies only slightly and is not as obvious as the alterations in temporal expression levels observed in the qRT-PCR data.

Sox10 (Figure 3A) – stage 25, unchanged; stage 30, slightly decreased; stage 34, significant decrease ($p=0.01$); stage 38, strong, 2 fold increase; stage 42, slightly increased; stage 45, unchanged.

In situ hybridization against *Sox10* in different developmental stages of FoxN3-depleted specimens reveals an almost unchanged spatial expression pattern compared to controls. *Sox10* is expressed in the neurocranium, otic capsule and weakly in ventral head region (Figure 3C). At stage 33/34 expression is less intense in the otic capsule and absent in the region dorsal to the eye in FoxN3-depleted embryos. Additionally, staining is vaguer and more condensed in the jaw and otic region and absent in the branchial region of FoxN3-depleted specimens at stage 39 (Figure 3C). The alteration of the spatial pattern matches the decreased expression level observed in the qRT-PCR data in FoxN3-depleted specimens at stage 34. However, the vaguer staining at around stage 39 is not mirrored in data from qRT-PCR.

Col2a1 (Figure 3A) – stage 25, significantly increased ($p=0.038$); stage 30, significantly decreased ($p=0.018$); stage 34, significantly decreased ($p=0.011$); stage 38, significantly decreased ($p=0.0023$); stage 42, significantly increased ($p=0.04$); stage 45, significantly decreased ($p=0.0001$).

In situ hybridization against *Col2a1* in different developmental stages of FoxN3-depleted specimens reveals some alterations of the spatial expression pattern compared to controls. In FoxN3-depleted specimens and controls, *Col2a1* is expressed in the developing branchial region, neurocranium and otic capsule (Figure 3D). At stage 31/32, staining against *Col2a1* is diffuse and slightly more intense around the eye of FoxN3-depleted specimens. At stage 33/34, staining is less intense in the branchial region. At stage 35/36 staining is less intense in the otic region. At stage 37/38 less intense in the branchial region of FoxN3-depleted specimens (Figure 3D). This pattern matches the general alterations in temporal expression levels observed in the qRT-PCR data.

Runx2 (Figure 4A) – stage 25, slightly increased; stage 30, significantly decreased ($p=0.009$); stage 34, slightly decreased; stage 38, significantly decreased ($p=0.001$); stage 42, significant twofold increase ($p=0.038$); stage 45, significant decrease ($p=0.008$).

In situ hybridization against *Runx2* in different developmental stages of FoxN3-depleted specimens reveals an almost similar but slightly more diffuse spatial expression pattern compared to controls (Figure 4B). At stage 35/36, staining is less intense in the developing cornua trabeculae of FoxN3-depleted specimens. At stage 35/36 and 39, the staining is less intense in the jaw and branchial region of FoxN3-depleted specimens. This pattern matches the alterations in temporal expression levels observed in the qRT-PCR data.

Xenopus hand 2 (*Xhand2*; Figure 4A) – stage 25, slightly decreased; stage 30, slightly increased; stage 34, significant increase ($p=0.01$); stage 38, significant decrease ($p=0.02$); stage 42, significant increase ($p=0.01$); stage 45, slightly increased.

In situ hybridization against *Xhand2* in different developmental stages of FoxN3-depleted specimens reveals an almost unchanged spatial expression pattern compared

to controls. *Xhand2* is expressed in the branchial region throughout all investigated stages (Figure 4C). Between stage 31 and 36 staining is more intense, at stage 37/38 less intense in FoxN3-depleted specimens compared to controls. This pattern is different compared to alterations in temporal expression levels. This difference might be due to the lower sensitivity of the *in situ* hybridisation compared to the qRT-PCR data.

Osteoblast specific transcription factor osterix (*Osx*; Figure 4A) – stage 25, slightly increased; stage 30, slightly decreased; stage 34, significant decrease ($p=0.007$); stage 38, unchanged; stage 42, slightly decreased; stage 45, slightly increased.

Morpholino-mediated knock-down of FoxN3 alters spatio-temporal expression patterns of genes involved in jaw joint formation

Gdf5 (Figure 5) – stage 25, significantly increased ($p=0.009$); stage 30, slightly increased; stage 34, significantly decreased ($p=0.0001$); stage 38 significantly 0.5 fold increase ($p=0.01$); stage 42, significant 3.25 fold increase ($p=0.019$); stage 45, significant decrease ($p=0.005$).

Gdf6 (Figure 5) – stage 25, slightly increased; stage 30, significant 0.8 fold decrease ($p=0.000006$); stage 34, unchanged; stage 38, slightly increased; stage 42, slightly decreased; stage 45, unchanged.

Distal-less 5 (*Dlx5*; Figure 5) – stage 25, significantly increased ($p=$); stage 30, slightly increased; stage 34, significantly decreased ($p=0.002$); stage 38, significant 0.75 fold decrease ($p=0.0002$); stage 42, significant slight decrease ($p=0.007$); stage 45, unchanged.

Dlx6 (Figure 5) – stage 25, unchanged; stage 30, unchanged; stage 34, significantly decreased ($p=0.008$); stage 38, significant 2.6 fold increase ($p=0.002$); stage 42, slightly decreased; stage 45, slightly increased.

Xbap (Figure 6A) – Primer and *in situ* probe were designed to bind to both variants of *Xbap*. Stage 25, significant decrease ($p=0.02$); stage 30, slightly increased; stage 34, unchanged; stage 38, slightly decreased; stage 42, significant 3.75 fold increase ($p=0.045$); stage 45, slightly decreased.

In situ hybridization against *Xbap* in different developmental stages of FoxN3-depleted specimens reveals spatial expression pattern similar to controls. *Xbap* is expressed in the otic capsule, jaw and branchial region (Figure 6B). This pattern matches the pattern of temporal expression levels observed in the qRT-PCR data.

Goosecoid (*gsc*; Figure 6A) – stage 25, significant 1.9 fold increase ($p=0.005$); stage 30, significant decrease ($p=0.02$); stage 34, slightly increased; stage 38, slightly decreased; stage 42, significant 2 fold increase ($p=0.008$); stage 45, slightly increased.

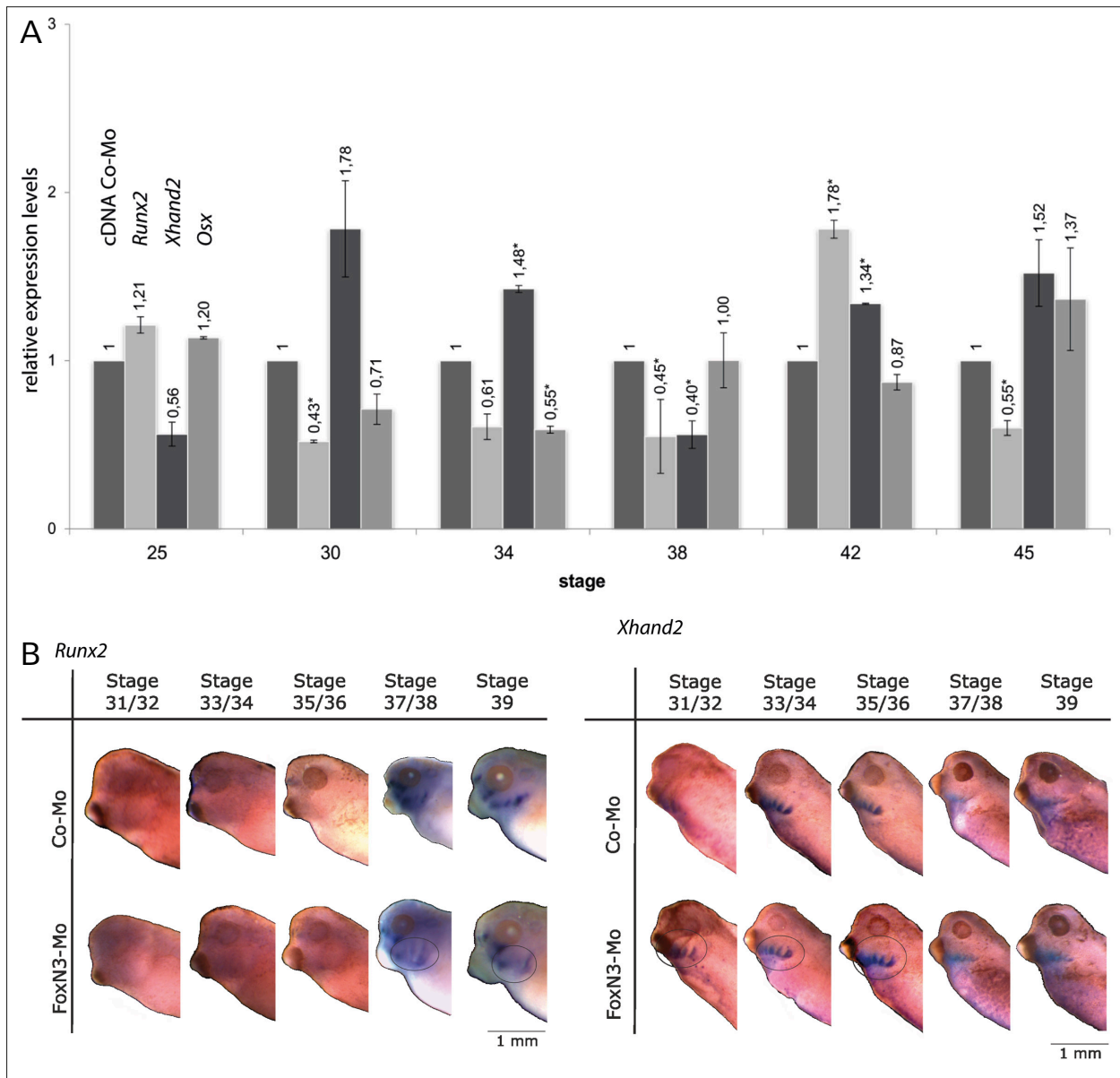


Fig. 4. Temporal and Spatial expression pattern of *Runx2*, *Xhand2* and *Osx* following knock-down of FoxN3. A, relative temporal expression patterns of *Runx2*, *Xhand2* and *Osx* in the head region of Co-Mo or FoxN3-Mo injected *Xenopus laevis*. Significant differences in gene expression levels between Co-Mo and FoxN3-Mo injected embryos are marked with an asterisk. B to C, Whole mount *in situ* hybridization against mRNA of different genes in the head region of Co-Mo and FoxN3 injected *X. laevis* at different developmental stages. Relevant region are indicated with a circle. B, *Runx2*. C, *Xhand2*.

Zampogna (*zax*; Figure 6A) – stage 25, significant increase ($p=0.018$); stage 30, slightly increased; stage 34, slightly increased; stage 38, slightly decreased; stage 42, significant increase ($p=0.016$); stage 45, significant decrease ($p=0.02$).

Morpholino-mediated knock-down of FoxN3 alters spatio-temporal expression patterns of genes involved in cranial myogenesis

Myf5 (Figure 7A) – stage 25, unchanged; stage 30, significant 2.2 fold increase ($p=0.037$); stage 34, slightly decreased; stage 38, slightly decreased; stage 42, significant decrease ($p=0.028$); stage 45, unchanged.

MyoD (Figure 7A) – stage 25, significant decrease ($p=0.009$); stage 30, slightly decreased; stage 34, significant 0.7 fold decrease ($p=0.0059$); stage 38, slightly decreased; stage 42, significant 2.2 fold increase ($p=0.013$); stage 45, slightly decreased.

In situ hybridization against *MyoD* in different developmental stages of FoxN3-depleted specimens reveals altered spatial expression pattern compared to controls. *MyoD* is expressed in the branchial and ventral head (Figure 7B). From stage 31 to 38, staining is less intense in FoxN3-depleted specimens. It is slightly more intense at stage 39. This pattern matches the alterations in temporal expression levels observed in the qRT-PCR data.

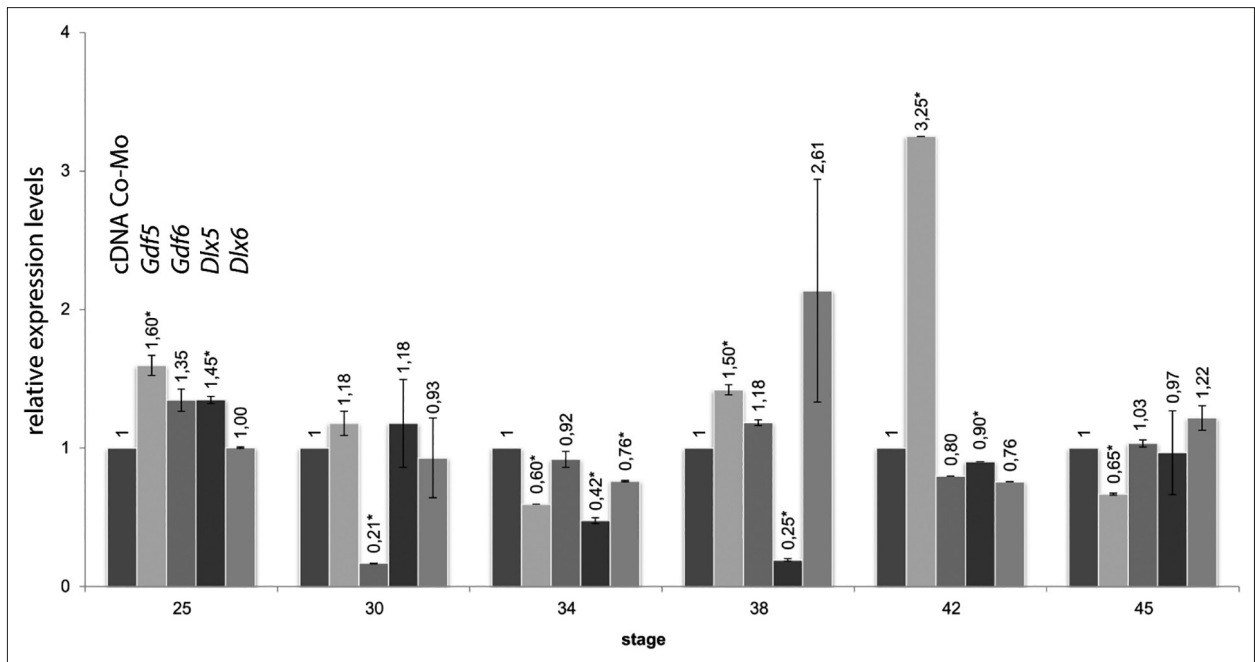


Fig. 5. Relative temporal expression pattern of *Gdf5*, *6* and *Dlx5*, *6* following knock-down of FoxN3. Significant differences in gene expression levels between Co-Mo and FoxN3-Mo injected embryos are marked with an asterisk.

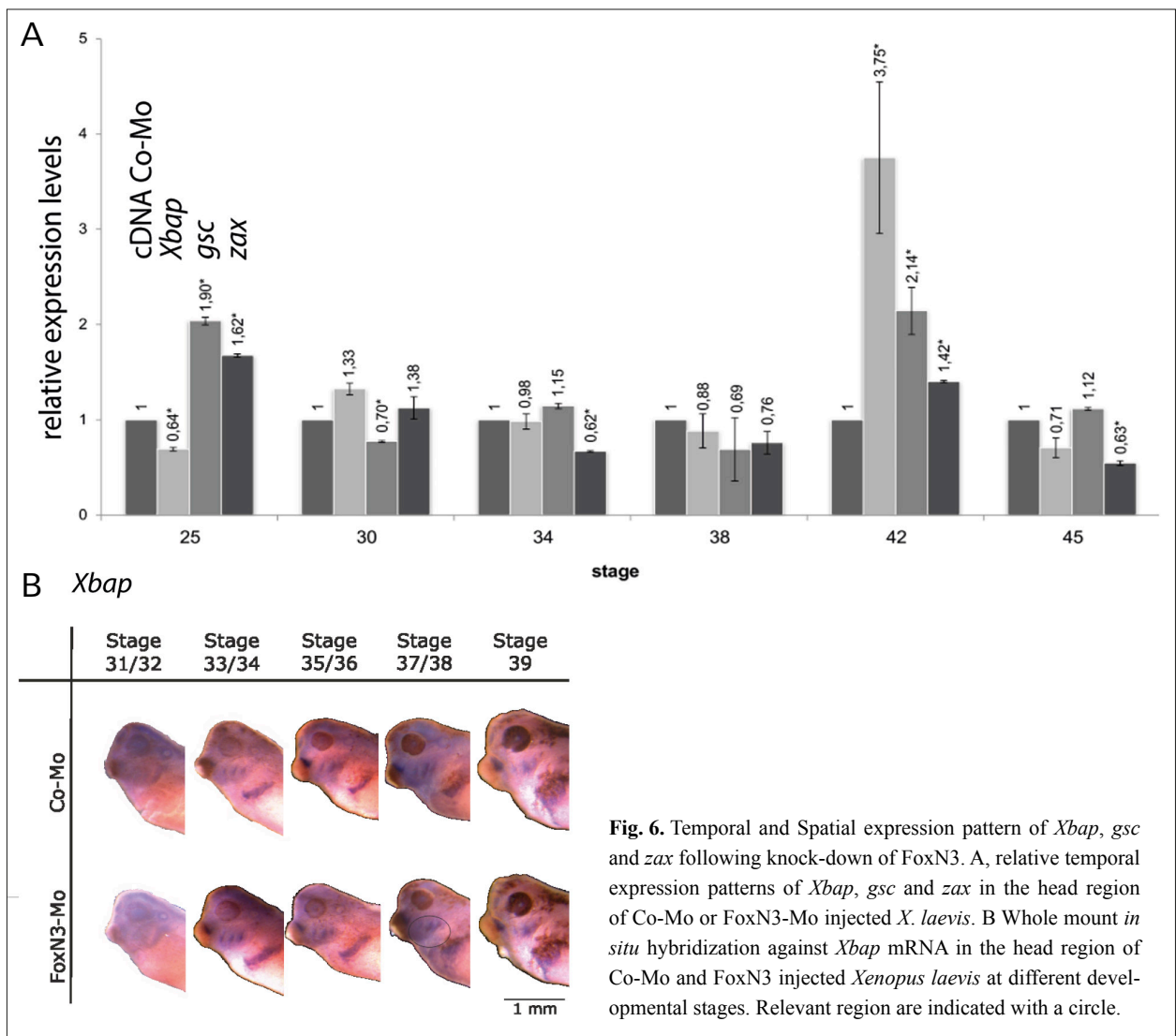


Fig. 6. Temporal and Spatial expression pattern of *Xbp*, *gsc* and *zax* following knock-down of FoxN3. A, relative temporal expression patterns of *Xbp*, *gsc* and *zax* in the head region of Co-Mo or FoxN3-Mo injected *X. laevis*. B Whole mount *in situ* hybridization against *Xbp* mRNA in the head region of Co-Mo and FoxN3 injected *Xenopus laevis* at different developmental stages. Relevant region are indicated with a circle.

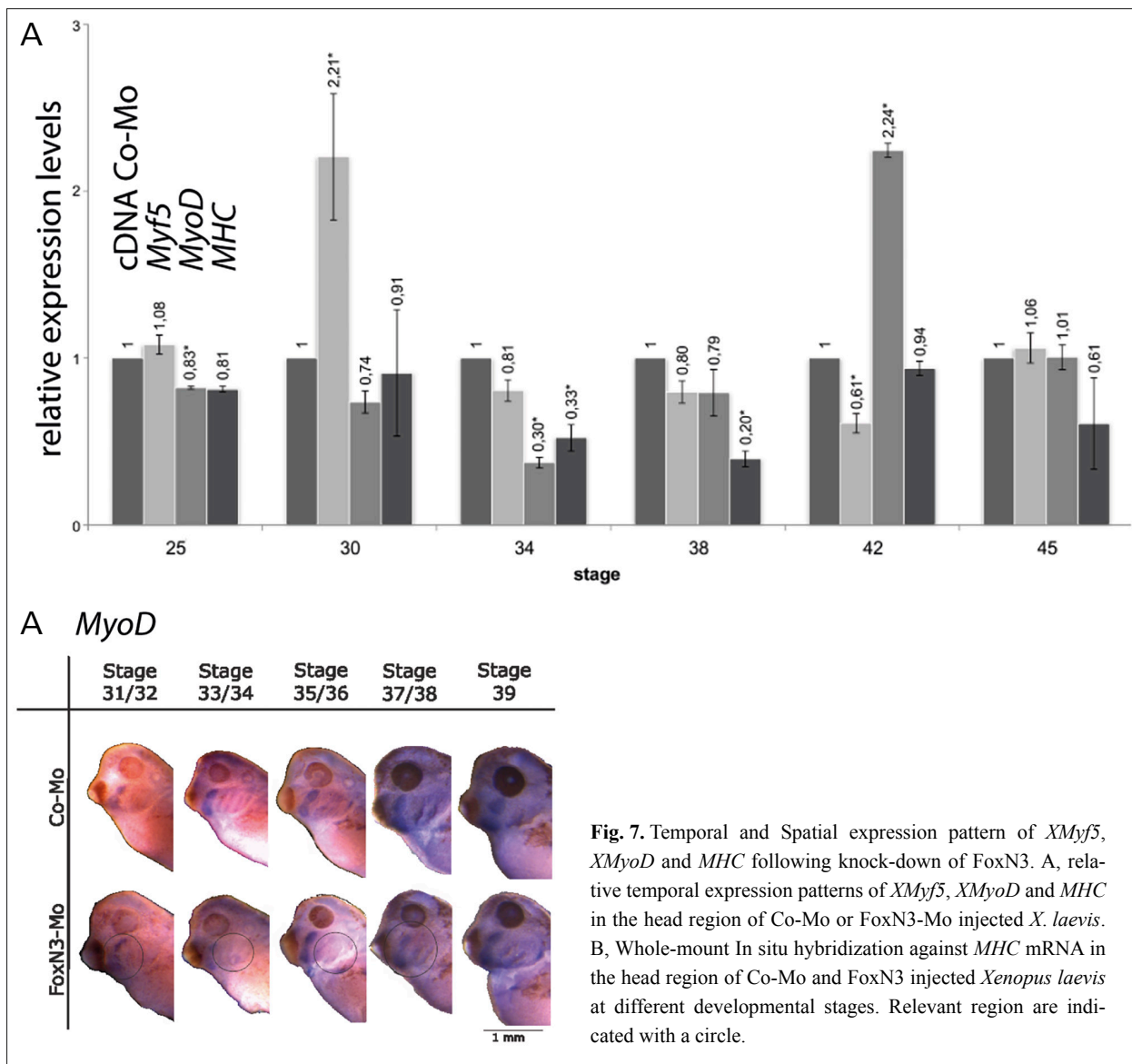


Fig. 7. Temporal and Spatial expression pattern of *XMyf5*, *XMyoD* and *MHC* following knock-down of FoxN3. A, relative temporal expression patterns of *XMyf5*, *XMyoD* and *MHC* in the head region of Co-Mo or FoxN3-Mo injected *X. laevis*. B, Whole-mount In situ hybridization against *MHC* mRNA in the head region of Co-Mo and FoxN3 injected *Xenopus laevis* at different developmental stages. Relevant region are indicated with a circle.

Myosin heavy chain (MHC; Figure 7A) – stage 25, slightly decreased; stage 30, unchanged; stage 34, significant decrease ($p=0.001$); stage 38, significant 0.8 fold decrease ($p=0.001$); stage 42 unchanged; stage 45, slightly decreased.

Discussion

FoxN3 regulates genes involved in early cell condensation formation during NC-derived cartilage development

In *X. laevis*, FoxN3 depletion results in a delayed and incomplete formation of NC-derived cartilages, whereas mesoderm-derived cartilages such as the basihyal, plana hyobranchiale, parachordals and otic capsule develop normally (SCHUFF *et al.*, 2007; SCHMIDT *et al.*, 2011,

2013). A summary of the qRT data from this study and key chondrogenic and myogenic events in “normal” and FoxN3-depleted *X. laevis* is given in Figure 8.

N-CAM and N-Cad

Following functional knock-down of *FoxN3* the cNCCs migrate normally from their origin among the hindbrain segments into the branchial arches (SCHUFF *et al.*, 2007) where some start to form pre-cartilaginous condensations (SCHMIDT *et al.*, 2011). Condensation initiation is characterized by an increased hyaluronidase activity and the appearance of cell adhesion molecules such as N-Cad, associated with the adhesion of cells in condensations, and N-CAM, mediating the maintenance of condensations via cell adhesion, aggregation and recruitment of mesenchymal cells (EDELMAAN, 1992; WIDELITZ *et al.*, 1993; HALL & MYAKE, 2000; DELISE & TUAN, 2002a, 2002b; GOLDRING *et al.*, 2006).

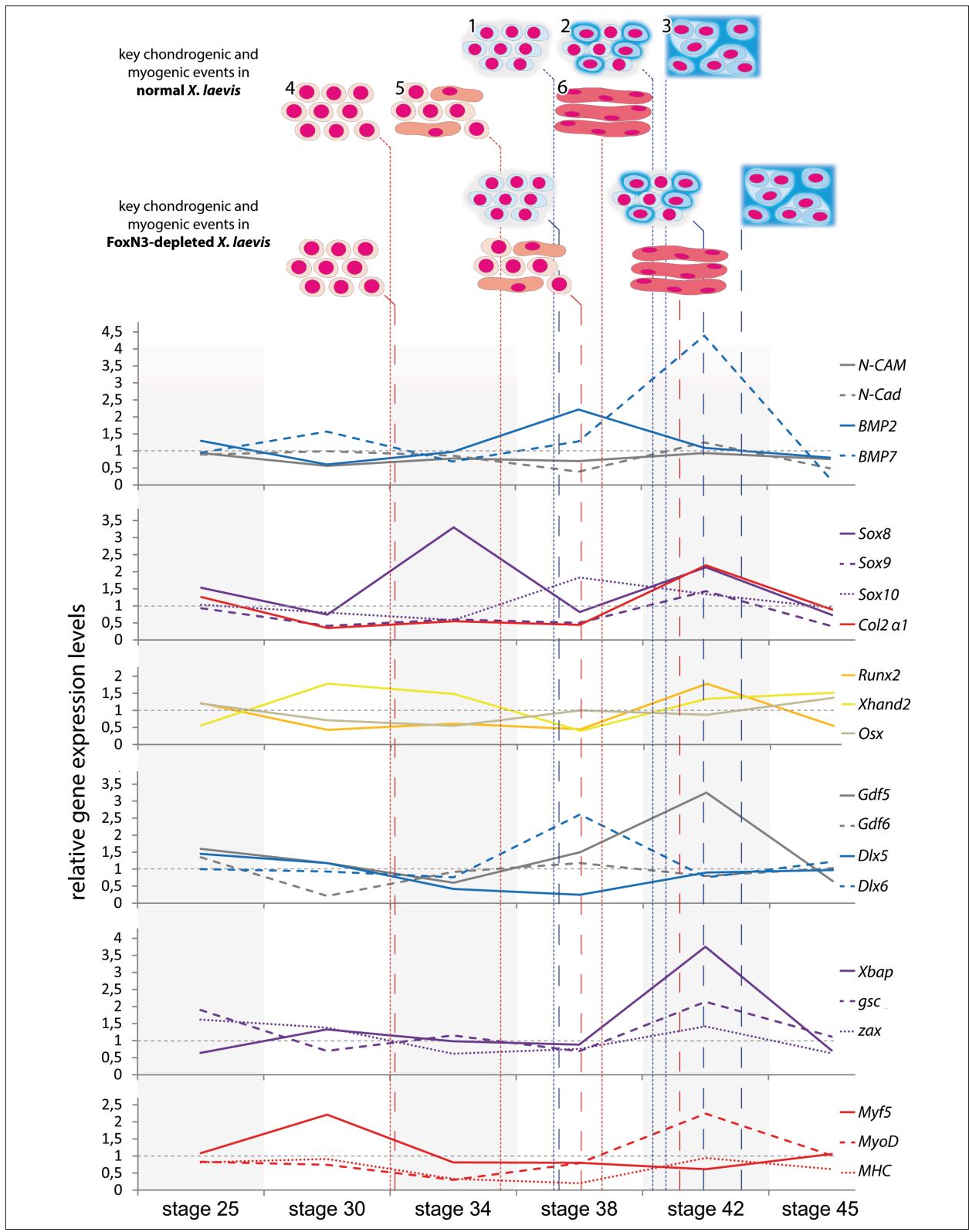


Fig. 8. Sequence of key chondrogenic and myogenic events in Co-Mo and FoxN3-Mo injected *X. laevis*. The events are plotted against the relative temporal expression levels of genes investigated in this study. In each graph, a dotted grey line indicates the “normal relative expression level” set to 1. The delay of later key chondrogenic and myogenic events in FoxN3-depleted *Xenopus laevis* matches the expression delay of associated genes compared to controls. Data on normal chondrocranial and muscle development are taken from ZIERMANN & OLSSON (2007); SCHMIDT *et al.* (2011) and LUKAS & OLSSON (2018a). Data on chondrocranial and muscle development in FoxN3-depleted specimens are taken from SCHMIDT *et al.* (2011) and the present study. 1, first pre-cartilaginous cell condensations are detectable; 2, first chondroblasts within condensations indicate the onset of cartilage differentiation; 3, chondrocytes are differentiated and most cartilaginous cranial skeletal elements are developed; 4, first pre-myogenic cell condensations are detectable; 5, first myocytes within condensations indicate the onset of muscle differentiation; 6, multinucleated myofibers are present and most cranial muscles are developed.

FoxN3-depleted tadpoles show weak condensation and smaller areas occupied by the condensations, as well as delayed differentiation resulting in smaller cartilages (SCHMIDT *et al.*, 2011). Our expression analysis shows that *N-CAM* and *N-Cad* are decreased in FoxN3-depleted specimens. This is similar to *N-CAM* antibody treated mesenchymal limb bud cells which result in delayed chondrification and condensations are only 68% of normal size (WIDELITZ *et al.*, 1993; DELISE & TUAN, 2002b). Furthermore, quantitative changes in *N-Cad* expression also perturb the morphogenesis of different tissues in *X. laevis* (FUJIMORI & TAKEICHI, 1993). In chicken, transfection of limb mesenchymal cell cultures with different deletion mutants of *N-Cad* results in significant decrease in cellular condensations, similar to the observed phenotype following FoxN3-depletion in *X. laevis* (FUJIMORI & TAKEICHI, 1993; DELISE & TUAN, 2002a, 2002b).

BMPs

BMP signalling is known to be important for NC formation. A knockout of *Bmp2/4* in chicken leads to hypomorphic branchial arches (FRANCIS-WEST *et al.*, 1994; BARLOW & FRANCIS-WEST, 1997; FRANCIS-WEST *et al.*, 1998). A *Bmp5/7* double knockout in mouse affects branchial arch outgrowth, implicating that application of BMPs or overexpression of BMPs can change skeletal patterning, resulting in, e.g., altered size and morphology (SOLLOWAY & ROBERTSON, 1999; KANZLER *et al.*, 2000). BMPs are necessary for different steps during cartilage formation by regulating transcription factors, such as *Sox9* or *Runx2*, as well as adhesion molecules [reviewed in (YOON & LYONS, 2004; NIE *et al.*, 2006)]. Therefore, BMPs are part of the instructive signals that promote commitment to a chondrogenic lineage. However, BMP-mediated gene regulation is more complex. A moderate increase in BMP expression maintains a chondrogenic cell lineage, but overexpression inhibits BMP2-induced chondrogenesis (HAAS & TUAN, 1999).

Our data show a decrease in BMP expressions in early stages followed by a twofold increase in BMP2 expression and a fourfold increase in BMP7 in FoxN3-depleted *X. laevis*. We argue that the early decrease in BMP expression following FoxN3 depletion disrupts the balanced signalling in the early steps of chondrogenesis. The transition from mesenchymal condensation to chondrocyte differentiation is characterised by the importance of a critical condensation size (HALL, 2005). Therefore, a decrease in cell-cell adhesion molecules may result in fewer cells being recruited to the developing condensation, poor growth of the condensation and a decrease in the area occupied by the condensation. The large increase in BMP expression in later stages can be interpreted as a compensation reaction as the fewer cells in the condensate try to restore the “normal” expression level.

Sox, *Runx2*, *Col2a1* and *Xhand2*

Further transcription factors are necessary for appropriate mesenchymal cell condensation, and for the regulation of extracellular matrix proteins. *Sox9* is one of the earliest known cartilage markers in vertebrates, directly regulating collagen type II and involved in pre-cartilaginous condensation formation (BELL *et al.*, 1997; BI *et al.*, 1999). Additionally, different other *Sox* genes have been shown to be redundant in function during NC development, such as *Sox8* and *Sox10* (HONG & SAINT-JEANNET, 2005). *Runx2* is a multifunctional transcription factor important for early mesenchyme condensation and larval hyobranchial formation in *X. laevis* (KOMORI, 2002; KERNEY *et al.*, 2007). The type II collagen protein starts to appear with the change in cellular phenotype from chondroblasts to proliferating chondrocytes.

Sox9 and *Col2a1* are expressed in the same regions of the forming craniofacial elements and the expression of both genes is decreased at stages 30-38 to less than half of control expression, followed by a twofold increase at stage 42 and again a decrease at stage 45 following FoxN3 depletion in *X. laevis*. *Runx2* expression follows a similar pattern in FoxN3-depleted tadpoles. The expression of *Sox10* is also decreased in early stages, but the expression of *Sox8* shows no permanent decrease. The *Sox10* expression increases earlier than *Sox9*, displaying a possible compensatory activity to the decrease in *Sox9* expression in early stages, as the alternating expression of *Sox8* also suggests. *Sox9* is also involved in the regulation of *Col2a1* expression as indicated by smaller skeletal elements, resulting from inappropriate condensation formation of NC-derived structures in a *Sox9* mutant mouse model (BELL *et al.*, 1997). *Sox9* knockout in cNCCs results in complete absence of cartilages and endochondral bones, whereas mesoderm-derived skeletal elements and intramembranous bones are normal (NG *et al.*, 1997; SPOKONY *et al.*, 2002; MORI-AKIYAMA *et al.*, 2003). A dominant negative form of *Runx2* inhibits the process of condensation and subsequent cartilaginous nodule formation in cultured vertebrate cells (AKIYAMA *et al.*, 1999), and a *Runx2*-Morpholino approach results in complete loss of cartilages in both zebrafish and *X. laevis* (FLORES *et al.*, 2006; KERNEY *et al.*, 2007). Additionally, overexpression of *XHand2*, known to be important for the development NC-derived structures, was found throughout development (NAKASHIMA *et al.*, 2002; YANAGISAWA, 2003). Overexpression of *Hand2* represses chondrogenesis and chondrogenic genes, such as *Sox9* and *collagen type II* (ABE *et al.*, 2010). FoxN3 depletion in *X. laevis* results in increased *Xhand2* expression at stages 30-34 and 42-45, which further explains the decrease in *Sox9* and *Col2a1* expression at these stages.

The direct relationship between *Sox*, as well as further transcription factors, and BMP signalling gives insights into the molecular regulation of the chondrogenic program (reviewed in YOON & LYONS, 2004). BMPs as well as TGF- β promote *Sox9* expression, and we found that BMPs as well as *Sox9*, *Col2a1* and *Runx2* decreased in

expression following functional knock-down of *FoxN3*. The observed phenotypes of FoxN3-depleted *X. laevis* can be explained by at least two different mechanisms that might interact during development.

1) FoxN3 regulates target gene expression directly or indirectly. Similarities in the observed phenotypes and the decreased *Bmp* expression in FoxN3-depleted *X. laevis* and *Sox9* mutant mice imply a possible regulation of *Sox9* by FoxN3, either directly or indirectly via BMP signalling. Furthermore, the condensation formation in FoxN3-depleted specimens start at stage 42, in controls at stage 39, and chondrocyte differentiation was first visible at stage 43 compared to stage 42 in controls. This mirrors the expression of the *Sox9*, *Col2a1* and *Runx2* genes in FoxN3-depleted *X. laevis*. FoxN3 might regulate the expression of genes necessary for cell-cell adhesion and for maintaining the critical expression levels necessary for cellular interactions during initiation of chondrogenesis. Furthermore, FoxN3 might play a prominent regulatory role in the signalling cascade during differentiation of NC-derived cartilages. Direct interaction of different *Fox* genes with BMP signalling was observed during neural plate and lateral mesoderm differentiation (MAHLAPUU *et al.*, 2001; NEILSON *et al.*, 2012). Studies on promoter regions in a subset of genes important for craniofacial development in mouse (*Bmp2*, 4, 7 and *Runx2*), showed the presence of a fork-head domain binding consensus sequence [(A/G)(T/C)AAA(C/T)A] (SAMAAAN *et al.*, 2010) giving further evidence for this scenario. It is known that the fork-head box proteins bind DNA as monomers and activate or repress the transcription either by regulating transcription independently, or by interacting with transcriptional regulators (CARLSSON & MAHLAPUU, 2002). Thus, *FoxN3* is a main regulator of chondrogenic initiation and further differentiation through direct (BMP signalling, *Runx2*) or indirect regulation (*Sox9*), which explains the phenotype of *FoxN3*-depleted tadpoles and the distinct expression patterns of different genes necessary for the formation of NC-derived cartilages.

2) FoxN3-depletion leads to an increase of cell death in early development and subsequent smaller progenitor populations. An alternative hypothesis of how FoxN3 depletion leads to the craniofacial defects was proposed by SCHUFF *et al.* (2007). *Ches1*, the yeast homolog of FoxN3, acts as a cell cycle checkpoint suppressor and promotes cell cycle arrest after DNA-damage at the transition from the G2- to the M-phase (PATI *et al.*, 1997). Yeast *Ches1* and *Xenopus* FoxN3 can bind to Sin3 and RPD3 proteins (SCHUFF *et al.*, 2007; SCOTT & PLOIN, 2003), both co-repressors of histone deacetylase complex (HDAC) (LADURON, 2004; SCHUFF *et al.*, 2007). HDAC is one of the major inhibitors of transcriptional activity by binding to DNA and promoting chromatin remodelling (JONES *et al.*, 1998; NAN *et al.*, 1998). However, HDAC alone does not interact with DNA but has to form protein complexes with, e.g., Sin3 to exert its inhibitory function (LADURON, 2004). Genomic as well as Morpholino medi-

ated knock-down of HDAC in the zebrafish, *Danio rerio*, leads to smaller eyes, craniofacial defects (especially in the mandibular and branchial arches), weak myocardia and prevented cardiac looping, as well as smaller fin buds (PILLAI *et al.*, 2004; YAMAGUCHI *et al.*, 2005). This phenotype is strikingly similar to the phenotypes produced by Morpholino mediated FoxN3 knock-down in *X. laevis* (SCHUFF *et al.*, 2007; ERICSSON *et al.*, 2009; SCHMIDT *et al.*, 2011; NAUMANN *et al.*, 2019). It was therefore proposed, that HDAC forms an active complex together with FoxN3, Sin3 and maybe RPD3, binding to the DNA via FoxN3 during the end of the G2-phase (SCHUFF *et al.*, 2007). The following chromatin remodelling inhibits transcription and leads to a stop at the checkpoint of the cell cycle to repair of DNA damage prior to DNA replication and mitotic cell division. After the knock-down of FoxN3, HDAC and its co-repressors Sin3 and RPD3 are unable to bind to the DNA and inhibit transcription. This prevents cell cycle stop at the G2/M-phase checkpoint leading to reduced time for DNA repair and subsequent accumulation of DNA damage. Programmed cell death, or apoptosis, removes cells with accumulated DNA damage, potentially harming the organism by turning into cancer cells (ROOS & KAINA, 2006). This interpretation gains support by the increased levels of apoptosis (SCHUFF *et al.*, 2007) and the decreased size of cranial cartilage and muscle anlagen (SCHMIDT *et al.*, 2011) in *FoxN3*-depleted *X. laevis*. Furthermore, this mechanistic hypothesis opens an alternative opportunity to explain the decreased expression levels of the investigated genes. Smaller anlagen with fewer cells lead to the lower expression levels detected by *in situ* hybridisation and qRT-PCR. During later developmental stages the fewer cells might try to compensate the lower cell number by the overexpression of the investigated genes. This hypothesis gains support by a study on the role of HDAC in NC-survival in *X. laevis* (RAO & LABONNE, 2018).

FoxN3 regulates genes involved in joint and head cartilage formation

In vertebrates, correct patterning of the jaw and branchial skeletal elements is controlled mainly by *Hox* genes expressed along the antero-posterior axis and *Dlx* genes expressed along the proximo-distal axis. The expression of *Dlx5/6* was decreased following FoxN3 depletion and the expression of *Xhand2* was increased at early stages, resulting in a change in regulation of intermediate elements and the joint. The palatoquadrate and Meckel's cartilage, including the primary jaw joint, develop exclusively from a ventral "mandibular" condensation, whereas the dorsal "maxillary" condensation gives rise to the trabecular cartilage and in anuran tadpoles to the supra-rostral cartilages (CERNY *et al.*, 2004). Following FoxN3 depletion, the palatoquadrate and Meckel's cartilages develop in proximity to each other and no joint is formed between them, so the tadpole cannot open its mouth. Different knock-out and overexpression studies describe

an interaction between *Hand2* and *Dlx5/6* expression (THOMAS *et al.*, 1998; YANAGISAWA, 2003). The resulting phenotypes show a hypoplastic jaw, fusion of Meckel's cartilage and the malleus, and a shortened tympanic ring (THOMAS *et al.*, 1998; YANAGISAWA, 2003). *Dlx5* knock-down using Morpholinos results in joint fusion and expansion of the expression domains of genes normally expressed in the intermediate area (TALBOT *et al.*, 2010). It seems possible that an increase in *Xhand2* expression following *FoxN3* depletion prevents the establishment of intermediate domain identity, as well as further regulation necessary for joint formation via the *Barx homeobox* gene. *Barx*, an inhibitor of *Xbap*, promotes cartilage development in the mandibular arch and inhibits joint development. During early patterning *Hand2* activates *barx* while both genes repress each other during cartilage differentiation (NICHOLS *et al.*, 2013). This later repressive interaction leads to the proper placement of the primary joint. Therefore, it is possible that during early development, the increase of *Xhand2* expression after FoxN3 knockdown leads to an increased *barx* expression. Later, during cartilage differentiation the previously increased *barx* expression may lead to a dorsal shift of *Xhand2* and the *barx* domains (ventral domain of the mandibular arch; CERNY *et al.*, 2010). The result could be a decrease or a shift of the *xbap* domain (ventral intermediate domain of the mandibular arch; CERNY *et al.*, 2010), resulting in joint loss. Additionally, the gene *Xbap* was shown to be required for formation of the jaw joint, the retroarticular process of Meckel's cartilage and the retroarticular bone, and is directly positively regulated by *Dlx5/6*, but inhibited by *Hand2* (MILLER, 2003; LUKAS & OLSSON, 2018b). Following functional knock-down of *FoxN3*, *Xbap* expression is decreased, suggesting that this results from a partial loss of intermediate identity. Moreover, expression of *Gdf5* and *Gdf6*, belonging to the earliest joint markers, is decreased at different stages following *FoxN3* depletion. *Gdf5* is directly regulated by *bapx* (EDWARDS & FRANCIS-WEST, 2001; WILSON & TUCKER, 2004). *Gdf5* knock-out mutants show no joint formation, and a mutation or Morpholino knock-down of *Bapx* also results in jaw joint loss in non-mammalian vertebrates (FRANCIS-WEST *et al.*, 1994; MILLER, 2003; SETTLE *et al.*, 2003; TUCKER *et al.*, 2004; LUKAS & OLSSON, 2018b). *Gdf6* has also been shown to be important for joint formation (SETTLE *et al.*, 2003). *FoxN3* depletion results in decreased expression of *Gdf6*.

The reduced expression of genes necessary for establishing the critical balance needed for normal jaw and branchial patterning following FoxN3 depletion, suggests that FoxN3 protein regulates the expression of genes necessary for the intermediate patterning of these structures. FoxN3 interacts with a component of the Sin3/Rpd3 HDAC complex, which is targeted to specific promoter regions via Sin3 interaction (SCOTT & PLON, 2003). The increased expression of *Xhand2* and decreased expression of genes further upstream is potentially due to loss of inhibition of the Sin3 complex via FoxN3 and possibly a direct inhibitory activity on *Xhand2*. This can in

turn lead to deacetylation of histones within promoters resulting in repression, as has been hypothesised for the reduction of osteogenic genes following Foxn3 mutation in mice (SAMAAAN *et al.*, 2010).

The patterning along the antero-posterior axis was not affected, except that the infrarostral cartilage was formed at the same level as Meckel's cartilage and not cranial to it. This resembles the anatomy of salamander larvae, which lack rostralia. The expression of *gsc* and *zax* is located mainly in the region of the infrarostral cartilage and the anterior part of Meckel's cartilage (NEWMAN *et al.*, 1997; NEWMAN & KRIEG, 1999). *FoxN3* depletion results in a decreased expression of both genes in this region, whereas expression of *zax* in the jaw and branchial region is unchanged. Additionally, the decrease in *zax* and *gsc* expression between stages 30 and 38 suggests that both genes are necessary for correct formation of the infrarostral and Meckel's cartilages. Furthermore, this indicates that both genes are needed to form the intermandibular commissure, which allows the cartilages to move relative to each other.

It has been suggested that these new structures are caused by gene duplication and diversification of gene function within the *bagpipe* genes (SVENSSON & HAAS, 2005). A *bagpipe* knock-out mouse mutant show malformation of first arch derivatives in the middle ear, and several bones at the base of the skull are also malformed (RIVERA-PÉREZ & MALLO, 1995; NEWMAN *et al.*, 1997). Moreover, *zax*-Morpholino injection causes a fatal deformation of the anterior part of the head and leads to missing rostralia in *X. laevis* (LUKAS *et al.*, 2020). A direct interaction between forkhead box transcription factors and homeoproteins is a general phenomenon in vertebrates and a direct interaction of *gsc* to a Fox protein was already examined (FOUCHER, 2003). Taken together, this suggests that a critical balance of expression of both *zax* and *gsc* is necessary for correct formation of the infrarostral cartilage and the intramandibular, possibly regulated through direct transcriptional control by *FoxN3*. This is in accordance with the idea that the evolution of new joints or cartilages (like the infrarostral cartilage) are rather due to changes in gene expression that regulate morphogenesis of skeletal elements than changes of gene expression necessary for early patterning (SQUARE *et al.*, 2015).

***FoxN3* affects directional guidance and morphogenesis of cranial muscles**

Following functional knock-down of *FoxN3* mandibular, hyoid, branchial and hyobranchial muscles are smaller, have a frayed appearance and several muscles are fused (the levator mandibulae muscle group, m. geniohyoideus and m. subarcualis rectus I, m. cucullaris) or show a shift in insertion (m. quadratohyoangularis and m. geniohyoideus). Eye and laryngeal muscles were not affected by functional knock-down of *FoxN3* (SCHUFF *et al.*, 2007; SCHMIDT *et al.*, 2011).

Myf5, *MyoD* and the structural muscle protein *MHC* (HOPWOOD *et al.*, 1991, 1992; CHANOINE & HARDY, 2003) are the first muscle specific genes to be expressed, and their activation is followed by the accumulation of transcripts of α -cardiac actin and larval myosin heavy chain transcripts (*MHC*) (CHANOINE & HARDY, 2003). The temporal expression levels of *Myf5*, *MyoD* and *MHC* are altered after *FoxN3* knock-down in *X. laevis*. The expression of *Myf5* was first increased and later slightly decreased following *FoxN3* depletion, but *MyoD* expression was decreased throughout development. *FoxN3* could have a direct regulatory role in *MyoD* and *Myf5* expression. *MyoD* and *Myf5* are expressed very early, at late blastula and gastrula stages, in response to mesoderm-inducing signals. However, transcription of *XMyoD* can only be induced during a very short period at early gastrula stages. This suggests that muscle induction is further controlled by mechanisms controlling the transcriptional responsiveness of the *XMyoD* gene locus. *XMyoD* induction was shown to be directly dependent upon histone deacetylase complex (HDAC) activity, whereas, except for *XMyoD*, the efficiency and timing of mesoderm induction events are independent of HDAC. A HDAC inhibition through Trichostatin-A treatment at early gastrula results in a significantly delayed and severely diminished *MyoD* expression in *X. laevis*, but the expression is not completely abolished (unpublished data). Expression of *Myf5* was less affected and only slightly reduced (STEINBACH *et al.*, 2000). Further muscle differentiation is characterised by myoblast fusion to form muscle fibers, where myoblast connection is mediated by glycoproteins, such as CAMs and Cadherins.

Reduced muscle formation could be explained by the drastic reduction (to 20-30% of control levels) in expression of *MHC*, the main structural protein of tadpole muscles, throughout development. Normal muscle development depends on a balance of signals provided by mesoderm cells as well as the surrounding cNCC-derived tissue at the right time and place in ontogeny. Therefore, inadequate development of cNCC-derived connective tissue surrounding the muscle fibers fails to support the signal transfer necessary for correct muscle fiber development. This result suggests that *FoxN3* has an (1) indirect effect on muscle morphogenesis due to its direct effect on the cNCC and its derivatives, resulting in incorrect muscle guidance from the origin to insertion and loose formation of muscle fibers and (2) possibly a direct effect on the early myogenic regulatory factor *MyoD*, resulting in decreased *MyoD* expression and inhibited muscle differentiation. This gains evidence by the similarity of observed phenotypes after *FoxN3* knock-down and cNCC extirpation experiments and also explains the normal development of NC-independent trunk and laryngeal muscles (SADAGHIANI & THIÉBAUD, 1987; ERICSSON *et al.*, 2004).

Acknowledgment

We thank B. Metscher and G. Müller (Vienna) for implementation of the X-ray based microcomputed tomography, and K. Felbel and B. Weiss for help with histological work, D. Siegel, C. Donow, N. Heymann, B. Korte, S. Schilling and L. Weilandt for help with *in situ* hybridization and qPCR. We are grateful to S. Eisenberg for help with animal care. We also thank the two anonymous reviewers for helpful comments on the manuscript.

Funding: This work was supported by the Deutsche Forschungsgemeinschaft (grant OL 134/2-4) to LO; and by the Konrad-Adenauer-Stiftung (stipend to JS).

References

- ABE, M., MICHIKAMI, I., FUKUSHI, T., ANE, A., MAEDA, Y., OOSHIMA, T. & WAKISAKA, S. (2010). Hand2 regulates chondrogenesis in vitro and in vivo. *Bone*, **46**, 1359–1368.
- AKIYAMA, H., KANNO, T., ITO, H. & TERRY, A. (1999). Positive and Negative Regulation of Chondrogenesis by Splice Variants of PEBP2A/CBF1 in Clonal Mouse EC Cells, ATDC5. *Journal of Cellular Physiology*, **181**, 169–178.
- BARLOW, A. & FRANCIS-WEST, P. (1997). Ectopic application of recombinant BMP-2 and BMP-4 can change patterning of developing chick facial primordia. *Development*, **398**, 391–398.
- BELL, D. M., LEUNG, K. K. H., WHEATLEY, S. C., NG, L. J., ZHOU, S., LING, K. W., SHAM, M. H., KOOPMAN, P., TAM, P. P. L. & CHEAH, K. S. E. (1997). SOX9 directly regulates the type-II collagen gene. *Nature Genetics*, **16**, 174–178.
- BI, W., DENG, J. M., ZHANG, Z., BEHRINGER, R. R. & DE CROMBRUGHE, B. (1999). Sox9 is required for cartilage formation. *Nature Genetics*, **22**, 85–89.
- CARLSSON, P. & MAHLAPUU, M. (2002). Forkhead transcription factors: key players in development and metabolism. *Developmental Biology*, **250**, 1–23.
- CERNY, R., LWIGALE, P., ERICSSON, R., MEULEMANS, D., EPPERLEIN, H.-H. & BRONNER-FRASER, M. (2004). Developmental origins and evolution of jaws: new interpretation of “maxillary” and “mandibular”. *Developmental Biology*, **276**, 225–236.
- CERNY, R., CATTELL, M., SAUKA-SPENGLER, T., BRONNER-FRASER, M., YU, F. & MEDEIROS, D. M. (2010). Evidence for the prepatterning/cooption model of vertebrate jaw evolution. *Proceedings of the National Academy of Sciences*, **107**, 17262–17267.
- CHANOINE, C. & HARDY, S. (2003). *Xenopus* muscle development: from primary to secondary myogenesis. *Developmental Dynamics*, **226**, 12–23.
- COULY, G. F., COLTEY, P. M. & LE DOUARIN, N. M. (1992). The developmental fate of the cephalic mesoderm in quail-chick chimeras. *Development*, **114**, 1–15.
- DAUDIN, F.-M. (1802). «An. XI». *Histoire Naturelle des Rainettes, des Grenouilles et des Crapauds. Quarto version*. Paris: Levraut.
- DELISE, A. M. & TUAN, R. S. (2002a). Alterations in the spatiotemporal expression pattern and function of N-cadherin inhibit cellular condensation and chondrogenesis of limb mesenchymal cells in vitro. *Journal of Cellular Biochemistry*, **87**, 342–359.
- DELISE, A. M. & TUAN, R. S. (2002b). Analysis of N-cadherin function in limb mesenchymal chondrogenesis in vitro. *Developmental Dynamics*, **225**, 195–204.

- DERVEAUX, S., VANDESOMPELE, J. & HELLEMANS, J. (2010). How to do successful gene expression analysis using real-time PCR. *Methods*, **50**, 227–230.
- EDELMAN G. M. (1992). Morphoregulation. *Developmental Dynamics*, **193**, 2–10.
- EDWARDS, C. J. & FRANCIS-WEST, P. H. (2001). Bone morphogenetic proteins in the development and healing of synovial joints. *Seminars in Arthritis and Rheumatism*, **31**, 33–42.
- ERICSSON, R., CERNY, R., FALCK, P. & OLSSON, L. (2004). Role of cranial neural crest cells in visceral arch muscle positioning and morphogenesis in the Mexican axolotl, *Ambystoma mexicanum*. *Developmental Dynamics*, **231**, 237–247.
- ERICSSON, R., ZIERMANN, J. M., PIEKARSKI, N., SCHUBERT, G., JOSS, J. & OLSSON, L. (2009). Cell fate and timing in the evolution of neural crest and mesoderm development in the head region of amphibians and lungfishes. *Acta Zoologica*, **90**, 264–272.
- FLORES, M. V., LAM, E. Y. N., CROSIER, P. & CROSIER, K. (2006). A hierarchy of Runx transcription factors modulate the onset of chondrogenesis in craniofacial endochondral bones in zebrafish. *Developmental Dynamics*, **235**, 3166–3176.
- FOUCHER, I. (2003). Joint regulation of the MAP1B promoter by HNF3beta/Foxa2 and Engrailed is the result of a highly conserved mechanism for direct interaction of homeoproteins and Fox transcription factors. *Development*, **130**, 1867–1876.
- FRANCIS-WEST, P. H., TATLA, T. & BRICKELL, P. M. (1994). Expression Patterns of the Bone Morphogenetic Protein Genes Bmp-4 and Bmp-2 in the Developing Chick Face Suggest a Role in Outgrowth of the Primordia. *Developmental Dynamics*, **201**, 168–178.
- FRANCIS-WEST, P. H., LADHER, R., BARLOW, A. & GRAVESON, A. (1998). Signalling interactions during facial development. *Mechanisms of Development*, **75**, 3–28.
- FUJIMORI, T. & TAKEICHI, M. (1993). Disruption of epithelial cell-cell adhesion by exogenous expression of a mutated nonfunctional N-cadherin. *Molecular Biology of the Cell*, **4**, 37–47.
- GANS, C. & NORTH CUTT, R. G. (1983). Neural crest and the origin of vertebrates: a new head. *Science*, **220**, 268–273.
- GOLDRING, M. B., TSUCHIMOTO, K. & IJIRI, K. (2006). The control of chondrogenesis. *Journal of Cellular Biochemistry*, **97**, 33–44.
- GRENIER, J., TEILLET, M.-A., GRIFONE, R., KELLY, R. G. & DUPREZ, D. (2009). Relationship between neural crest cells and cranial mesoderm during head muscle development. *PLoS One*, **4**, e4381.
- HAAS, A. R. & TUAN, R. S. (1999). Chondrogenic differentiation of murine C3H10T1/2 multipotential mesenchymal cells: II. Stimulation by bone morphogenetic protein-2 requires modulation of N-cadherin expression and function. *Differentiation*, **64**, 77–89.
- HALL, B. K. (2005). *Bones and Cartilage*. Elsevier Academic Press.
- HALL, B. K. (2009). *The Neural Crest and Neural Crest in Vertebrate Development and Evolution*. Springer.
- HALL, B. K. & MIYAKE, T. (1992). The membranous skeleton: the role of cell condensations in vertebrate skeletogenesis. *Anatomy and Embryology*, **186**, 107–124.
- HALL, B. K. & MIYAKE, T. (1995). Divide, accumulate, differentiate: cell condensation in skeletal development revisited. *Developmental Biology*, **39**, 881–893.
- HALL, B. K. & MIYAKE, T. (2000). All for one and one for all: condensations and the initiation of skeletal development. *Bioessays*, **22**, 138–47.
- HARLAND, R. M. (1991). In situ hybridization: an improved whole-mount method for *Xenopus* embryos. *Methods in Cell Biology*, **36**, 685–695.
- HONG, C.-S. & SAINT-JEANNET, J.-P. (2005). Sox proteins and neural crest development. *Seminars in Cell & Developmental Biology*, **16**, 694–703.
- HOPWOOD, N. D., PLUCK, A. & GURDON, J. B. (1991). *Xenopus* Myf-5 marks early muscle cells and can activate muscle genes ectopically in early embryos. *Development*, **111**, 551–560.
- HOPWOOD, N. D., PLUCK, A., GURDON, J. B. & DILWORTH, S. M. (1992). Expression of XMyoD protein in early *Xenopus laevis* embryos. *Development*, **114**, 31–38.
- JONES, P. L., VEENSTRA, G. J. C., WADE, P. A., VERMAAK, D., KASS, S. U., LANDSBERGER, N., STROUBOULIS, J. & WOLFFE, A. P. (1998). Methylated DNA and MeCP2 recruit histone deacetylase to repress transcription. *Letters to Nature*, **19**, 187–191.
- KANZLER, B., FOREMAN, R. K., LABOSKY, P. A. & MALLO, M. (2000). BMP signaling is essential for development of skeletogenic and neurogenic cranial neural crest. *Development*, **127**, 1095–1104.
- KERNEY, R., GROSS, J. B. & HANKEN, J. (2007). Runx2 is essential for larval hyobranchial cartilage formation in *Xenopus laevis*. *Developmental Dynamics*, **236**, 1650–1662.
- KOMORI, T. (2002). Runx2, a multifunctional transcription factor in skeletal development. *Journal of Cellular Biochemistry*, **87**, 1–8.
- LADURON, S. (2004). MAGE-A1 interacts with adaptor SKIP and the deacetylase HDAC1 to repress transcription. *Nucleic Acids Research*, **32**, 4340–4350.
- LE DOUARIN, N. M., ZILLER, C. & COULY, G. F. (1993). Patterning of Neural Crest Derivatives in the Avian Embryo - in-Vivo and in-Vitro Studies. *Developmental Biology*, **159**, 24–49.
- LE LIÈVRE, C. S. & LE DOUARIN, N. M. (1975). Mesenchymal derivatives of the neural crest: analysis of chimaeric quail and chick embryos. *Journal of Embryology and Experimental Morphology*, **34**, 125–154.
- LU, J.-R., BASSEL-DUBY, R., HAWKINS, A., CHANG, P., VALDEZ, R., WU, H., GAN, L., SHELTON, J. M., RICHARDSON, J. A. & OLSON, E. N. (2002). Control of facial muscle development by MyoR and capulin. *Science*, **298**, 2378–2381.
- LUKAS, P. & OLSSON, L. (2018a). Sequence and timing of early cranial skeletal development in *Xenopus laevis*. *Journal of Morphology*, **279**, 62–74.
- LUKAS, P. & OLSSON, L. (2018b). Bapx1 is required for jaw joint development in amphibians. *Evolution and Development*, **20**, 192–206.
- LUKAS, P., SCHMIDT, J. & OLSSON, L. (2020). Knockdown of zax in *Xenopus laevis* leads to craniofacial malformations and the absence of the intramandibular joint. *Vertebrate Zoology*, **70**, 9–22.
- MAHLAPUU, M., ORMESTAD, M., ENERBÄCK, S. & CARLSSON, P. (2001). The forkhead transcription factor Foxf1 is required for differentiation of extra-embryonic and lateral plate mesoderm. *Development*, **128**, 155–166.
- MILLER, C. T. (2003). Two endothelin 1 effectors, hand2 and bapx1, pattern ventral pharyngeal cartilage and the jaw joint. *Development*, **130**, 1353–1365.
- MORI-AKIYAMA, Y., AKIYAMA, H., ROWITCH, D. H. & DE CROMBRUGGHE, B. (2003). Sox9 is required for determination of the chondrogenic cell lineage in the cranial neural crest. *PNAS*, **100**, 9360–9365.
- NAKASHIMA, K., ZHOU, X., KUNKEL, G., ZHANG, Z., DENG, J. M., BEHRINGER, R. R. & DE CROMBRUGGHE, B. (2002). The novel zinc finger-containing transcription factor osterix is required for osteoblast differentiation and bone formation. *Cell*, **108**, 17–29.
- NAN, X., NG, H. H., JOHNSON, C. A., LAHERTY, C. D., TURNER, B. M., EISENMAN, R. N. & BIRD, A. (1998). Transcriptional repression by the methyl-CpG-binding protein MeCP2 involves a histone deacetylase complex. *Nature*, **393**, 386–389.
- NAUMANN, B., SCHMIDT, J. & OLSSON, L. (2019). FoxN3 is necessary for the development of the interatrial septum, the ventricular trabeculae and the muscles at the head/trunk interface in the African clawed frog, *Xenopus laevis* (Lissamphibia: Anura: Pipidae). *Developmental Dynamics*, **248**, 323–336.
- NEILSON, K. M., KLEIN, S. L., MHASKE, P., MOOD, K., DAAR, I. O. & MOODY, S. A. (2012). Specific domains of FoxD4/5 activate and repress neural transcription factor genes to control the progression of immature neural ectoderm to differentiating neural plate. *Developmental Biology*, **365**, 363–375.
- NEWMAN, C. S., GROW, M. W., CLEAVER, O., CHIA, F. & KRIEG, P. (1997). Xbap, a vertebrate gene related to bagpipe, is expressed in developing craniofacial structures and in anterior gut muscle. *Developmental Biology*, **181**, 223–233.

- NEWMAN, C. S. & KRIEG, P. A. (1999). The *Xenopus* bagpipe-related homeobox gene *zampogna* is expressed in the pharyngeal endoderm and the visceral musculature of the midgut. *Development Genes and Evolution*, **209**, 132–134.
- NG, L. J., WHEATLEY, S., MUSCAT, G. E., CONWAY-CAMPBELL, J., BOWLES, J., WRIGHT, E., BELL, D. M., TAM, P. P., CHEAH, K. S. & KOOPMAN, P. (1997). SOX9 binds DNA, activates transcription, and coexpresses with type II collagen during chondrogenesis in the mouse. *Developmental Biology*, **183**, 108–121.
- NICHOLS, J. T., PAN, L., MOENS, C. B. & KIMMEL, C. B. (2013). *barx1* represses joints and promotes cartilage in the craniofacial skeleton. *Development*, **140**, 2765–2775.
- NIE, X., LUUKKO, K. & KETTUNEN, P. (2006). BMP signalling in craniofacial development. *Developmental Biology*, **50**, 511–521.
- NIEUWKOOP, P. D. & FABER, J. (1994). *Normal table of Xenopus laevis (Daudin) A systematical and chronological survey of the development from the fertilized egg till the end of metamorphosis*. Garland Pub.
- NODEN, D. M. (1983). The embryonic origins of avian cephalic and cervical muscles and associated connective tissues. *Journal of Anatomy*, **168**, 257–276.
- NODEN, D. M. (1983). The role of the neural crest in patterning of avian cranial skeletal, connective, and muscle. *Developmental Biology*, **96**, 144–165.
- OLSSON, L., FALCK, P., LOPEZ, K., COBB, J. & HANKEN, J. (2001). Cranial neural crest cells contribute to connective tissue in cranial muscles in the anuran amphibian, *Bombina orientalis*. *Developmental Biology*, **237**, 354–367.
- PATI, D., KELLER, C., GROUDINE, M. & PLON, S. E. (1997). Reconstitution of a MEC1-independent checkpoint in yeast by expression of a novel human fork head cDNA. *Molecular and Cellular Biology*, **17**, 3037–3046.
- PILLAI, R., COVERDALE, L. E., DUBEY, G. & MARTIN, C. C. (2004). Histone deacetylase 1 (HDAC-1) required for the normal formation of craniofacial cartilage and pectoral fins of the zebrafish. *Developmental Dynamics*, **231**, 647–654.
- RAO, A. & LABONNE, C. (2018). Histone deacetylase activity has an essential role in establishing and maintaining the vertebrate neural crest. *Development*, **145**.
- RINON, A., LAZAR, S., MARSHALL, H., BÜCHMANN-MÖLLER, S., NEUFELD, A., ELHANANY-TAMIR, H., TAKETO, M. M., SOMMER, L., KRUMLAUF, R. & TZAHOR, E. (2007). Cranial neural crest cells regulate head muscle patterning and differentiation during vertebrate embryogenesis. *Development*, **134**, 3065–3075.
- RIVERA-PÉREZ, J. & MALLO, M. (1995). Goosecoid is not an essential component of the mouse gastrula organizer but is required for craniofacial and rib development. *Development*, **121**, 3005–3012.
- ROMEIS, B. (2007). *Romeis - Mikroskopische Technik* (M. Mulisch & U. Welsch (eds.); 18th ed.). Spektrum Akademischer Verlag.
- ROOS, W. P. & KAINA, B. (2006). DNA damage-induced cell death by apoptosis. *Trends in Molecular Medicine*, **12**, 440–450.
- SADAGHIANI, B. & THIÉBAUD, C. H. (1987). Neural crest development in the *Xenopus laevis* embryo, studied by interspecific transplantation and scanning electron microscopy. *Developmental Biology*, **124**, 91–110.
- SAMAAN, G., YUGO, D., RAJAGOPALAN, S., WALL, J., DONNELL, R., GOLDOWITZ, D., GOPALAKRISHNAN, R. & VENKATACHALAM, S. (2010). Foxn3 is essential for craniofacial development in mice and a putative candidate involved in human congenital craniofacial defects. *Biochemical and Biophysical Research Communications*, **400**, 60–65.
- SATOH, A., SUZUKI, M., AMANO, T., TAMURA, K. & IDE, H. (2005). Joint development in *Xenopus laevis* and induction of segmentations in regenerating froglet limb (spike). *Developmental Dynamics*, **233**, 1444–1453.
- SCHMIDT, J., PIEKARSKI, N. & OLSSON, L. (2013). Cranial muscles in amphibians: development, novelties and the role of cranial neural crest cells. *Journal of Anatomy*, **222**, 134–146.
- SCHMIDT, J., SCHUFF, M. & OLSSON, L. (2011). A role for FoxN3 in the development of cranial cartilages and muscles in *Xenopus laevis* (Amphibia: Anura: Pipidae) with special emphasis on the novel rostral cartilages. *Journal of Anatomy*, **218**, 226–242.
- SCHUFF, M., RÖSSNER, A., DONOW, C. & KNÖCHEL, W. (2006). Temporal and spatial expression patterns of FoxN genes in *Xenopus laevis* embryos. *The International Journal of Developmental Biology*, **50**, 429–434.
- SCHUFF, M., RÖSSNER, A., WACKER, S. A., DONOW, C., GESSERT, S. & KNÖCHEL, W. (2007). FoxN3 is required for craniofacial and eye development of *Xenopus laevis*. *Developmental Dynamics*, **236**, 226–239.
- SCOTT, K. L. & PLON, S. E. (2003). Loss of Sin3/Rpd3 histone deacetylase restores the DNA damage response in checkpoint-deficient strains of *Saccharomyces cerevisiae*. *Molecular and Cellular Biology*, **23**, 4522.
- SETTLE, S. H., ROUNTREE, R. B., SINHA, A., THACKER, A., HIGGINS, K. & KINGSLEY, D. M. (2003). Multiple joint and skeletal patterning defects caused by single and double mutations in the mouse Gdf6 and Gdf5 genes. *Developmental Biology*, **254**, 116–130.
- SOLLOWAY, M. J. & ROBERTSON, E. J. (1999). Early embryonic lethality in Bmp5; Bmp7 double mutant mice suggests functional redundancy within the 60A subgroup. *Development*, **126**, 1753–1768.
- SPOKONY, R. F., AOKI, Y., SAINT-GERMAIN, N., MAGNER-FINK, E. & SAINT-JEANNET, J.-P. (2002). The transcription factor Sox9 is required for cranial neural crest development in *Xenopus*. *Development*, **129**, 421–432.
- SQUARE, T., JANDZIK, D., CATTELL, M., COE, A., DOHERTY, J. & MEDEIROS, D. M. (2015). A gene expression map of the larval *Xenopus laevis* head reveals developmental changes underlying the evolution of new skeletal elements. *Developmental Biology*, **397**, 293–304.
- STEINBACH, O. C., WOLFFE, A. P. & RUPP, R. A. (2000). Histone deacetylase activity is required for the induction of the MyoD muscle cell lineage in *Xenopus*. *Journal of Biological Chemistry*, **381**, 1013–1016.
- SVENSSON, M. E. & HAAS, A. (2005). Evolutionary innovation in the vertebrate jaw: A derived morphology in anuran tadpoles and its possible developmental origin. *Bioessays*, **27**, 526–532.
- TALBOT, J. C., JOHNSON, S. L. & KIMMEL, C. B. (2010). hand2 and Dlx genes specify dorsal, intermediate and ventral domains within zebrafish pharyngeal arches. *Development*, **137**, 2507–2517.
- THOMAS, T., KURIHARA, H., YAMAGISHI, H., KURIHARA, Y., YAZAKI, Y., OLSON, E. N. & SRIVASTAVA, D. (1998). A signaling cascade involving endothelin-1, dHAND and msx1 regulates development of neural-crest-derived branchial arch mesenchyme. *Development*, **125**, 3005–3014.
- TUCKER, A. S., WATSON, R. P., LETTICE, L. A., YAMADA, G. & HILL, R. E. (2004). Bapx1 regulates patterning in the middle ear: altered regulatory role in the transition from the proximal jaw during vertebrate evolution. *Development*, **131**, 1235–1245.
- WIDELITZ, R. B., JIANG, T. X., MURRAY, B. A. & CHUONG, C. M. (1993). Adhesion molecules in skeletogenesis: II. Neural cell adhesion molecules mediate. *Journal of Cellular Physiology*, **156**, 399–411.
- WILSON, J. A. & TUCKER, A. S. (2004). Fgf and Bmp signals repress the expression of Bapx1 in the mandibular mesenchyme and control the position of the developing jaw joint. *Developmental Biology*, **266**, 138–150.
- YAMAGUCHI, M., TONOU-FUJIMORI, N., KOMORI, A., MAEDA, R., NOJIMA, Y., LI, H., OKAMOTO, H. & MASAI, I. (2005). Histone deacetylase 1 regulates retinal neurogenesis in zebrafish by suppressing Wnt and Notch signaling pathways. *Development*, **132**, 3027–3043.
- YANAGISAWA, H. (2003). Targeted deletion of a branchial arch-specific enhancer reveals a role of dHAND in craniofacial development. *Development*, **130**, 1069–1078.
- YOON, B. S. & LYONS, K. M. (2004). Multiple functions of BMPs in chondrogenesis. *Journal of Cellular Biochemistry*, **93**, 93–103.
- ZIERMANN, J. M. & OLSSON, L. (2007). Patterns of spatial and temporal cranial muscle development in the African clawed frog, *Xenopus laevis* (Anura: Pipidae). *Journal of Morphology*, **268**, 791–804.

Appendix

Supplementary material 1: List of Primer Pair Sequences and Annealing temperatures used for qRT-PCR. Denaturation temperature was set to 95°C and extension temperature was set to 72°C.

| Primer | Sequence Forward Primer (5'® 3) | Sequence Reverse Primer (5'® 3) | Annealing temperature (°C)/time (s) |
|---------------|------------------------------------|------------------------------------|--|
| <i>N-CAM</i> | GCCAGAACTTGGTGA | TTCTGTGAAGCTGTC | 54/20 |
| <i>N-Cad</i> | AAGTTTTCAATAAGCA | TGGTACATTAATAACC | 58 /20 |
| <i>Bmp-2</i> | AAGTTTTGATGCCGGC | CACTTCAACACCATGG | 56/5 |
| <i>Bmp-7</i> | TGTACGTCAGACCTTG | TCACAGTAAATATCCC | 56/5 |
| <i>Sox-8</i> | GGGCATCTCCAAACGGG | CTTGGGACACCTCGAA | 54/5 |
| <i>Sox-9</i> | GCTGAAGAAGGGAGGA | ATATCCCTTCTGGCTG | 53/5 |
| <i>Sox-10</i> | GCCTCAC TGGTAGCAG | TGCCACAGTTTGTTC | 56/5 |
| <i>Col2a1</i> | TGCTTTTGCTTCTCAA | GGAGAGAGTTTGGTC | 54/5 |
| <i>Runx2</i> | CGCCACCTATGAGCAA | GAGTCATCAACTGTGC | 56/5 |
| <i>Xhand2</i> | CCTTATTTTCTGGCTA | GGCTGTAGGATGCCAT | 56/5 |
| <i>Dlx-5</i> | AATGGTAAATGAAGAA | CTGCGAGTTGCTGGAG | 58/20 |
| <i>Dlx-6</i> | CGCTTCCAGCACCCAA | CCCAAAGAAGCGGCC | 54/20 |
| <i>Gdf-5</i> | CCGGCGAACAAAATCC | GACCTCCCATTATCAA | 55/20 |
| <i>Gdf-6</i> | AGCTCARCATGAAGGG | TAATGGCATGGGTGGG | 54/20 |
| <i>Xbap</i> | GCCACACGTTCCCCAG | TCCTTCTGCTCTCCC | 54/5 |
| <i>Gsc</i> | GATGCCCGCCAGTGCCTC | TGCAGCTCAGTTCGTGACAAA | 54/5 |
| <i>Zax</i> | CGGCGGTACACAAGAG | GCACCCTGACCACCTT | 56/5 |
| <i>Myf5</i> | TATCACCCCGCCAGTA | GATTGGTCGGTCATGC | 52/20 |
| <i>MyoD</i> | AGCGTTTGAGACCCTGAAGC | TATGTAGCGAATCGCGTTGC | 56/5 |
| <i>MHC</i> | GGCTGTTCGAGGCTGTAAATGC | TAGGTCCACCATTAGATCCTCGATT | 54/5 |
| <i>H4</i> | GGCAAAGGAGGAAAAGGACTG | GGTGATGCCCTGGATGTTGT | 54/5 |